Recent loss of the Dim2 DNA methyltransferase decreases mutation rate in repeats and changes evolutionary trajectory in a fungal pathogen

Mareike Möller[1,2,#*], Michael Habig[1,2], Cécile Lorrain[1,2], Alice Feurtey[1,2], Janine Haueisen[1,2], Wagner C. Fagundes[1,2], Alireza Alizadeh[3], Michael Freitag[4], Eva H. Stukenbrock[1,2*]

[1]Environmental Genomics, Christian-Albrechts University, Am Botanischen Garten 1-9, D-24118 Kiel, Germany

[2]Max Planck Institute for Evolutionary Biology, August-Thienemann-Str. 2, D-24306 Plön, Germany

[3]Department of Plant Protection, Faculty of Agriculture, Azarbaijan Shahid Madani University, Tabriz, Iran

[4]Department of Biochemistry and Biophysics, Oregon State University, Corvallis, OR, United States of America

*Corresponding authors
Eva H. Stukenbrock (estukenbock@uni-kiel.de)
Mareike Möller (moellmar@oregonstate.edu)

[#]Current address: Department of Biochemistry and Biophysics, Oregon State University, Corvallis, OR, United States of America

Keywords
DNA methylation, genome evolution, transposable elements, experimental evolution, fungal pathogen

Abstract

DNA methylation is found throughout all domains of life, yet the extent and function of DNA methylation differ between eukaryotes. Strains of the plant pathogenic fungus *Zymoseptoria tritici* appeared to lack cytosine DNA methylation (5mC) because gene amplification followed by Repeat-Induced Point mutation (RIP) resulted in the inactivation of the *dim2* DNA methyltransferase gene. 5mC is, however, present in closely related sister species. We demonstrate that inactivation of *dim2* occurred recently as some *Z. tritici* isolates carry a functional *dim2* gene. Moreover, we show that *dim2* inactivation occurred by a different path than previously hypothesized. We mapped the genome-wide distribution of 5mC in strains with and without functional *dim2*. Presence of functional *dim2* correlates with high levels of 5mC in transposable elements (TEs), suggesting a role in genome defense. We identified low levels of 5mC in strains carrying inactive *dim2* alleles, suggesting that 5mC is maintained over time, presumably by an active Dnmt5 DNA methyltransferase. Integration of a functional *dim2* allele in strains with mutated *dim2* restored normal 5mC levels, demonstrating *de novo* cytosine methylation activity of *dim2*. To assess the importance of 5mC for genome evolution, we performed an evolution experiment, comparing genomes of strains with high levels of 5mC to genomes of strains lacking *dim2*. We found that the presence of *dim2* alters nucleotide composition by promoting C to T transitions (C→T) specifically at CpA (CA) sites during mitosis, likely contributing to TE inactivation. Our results show that 5mC density at TEs is a polymorphic trait in *Z. tritici* populations that can impact genome evolution.

Author Summary

Cytosine DNA methylation (5mC) is known to silence transposable elements in fungi and thereby appears to contribute to genome stability. The genomes of plant pathogenic fungi are highly diverse, differing substantially in transposon content and distribution. Here, we show extensive differences of 5mC levels within a single species of an important wheat pathogen. These differences were caused by inactivation of the DNA methyltransferase Dim2 in the majority of studied isolates. Presence of widespread 5mC increased point mutation rates in regions with active or mutated transposable elements during mitosis. The mutation pattern is dependent on the presence of Dim2 and resembles a mitotic version of Repeat-Induced Point mutation (RIP). Thus, loss of 5mC may represent an evolutionary trade-off offering adaptive potential at the cost of transposon control.

Introduction

DNA methylation is an important process for epigenetic regulation, and functions range from dynamic control of gene expression to transposon silencing and the maintenance of genome integrity [1,2]. Although DNA methylation has been detected on both cytosines and adenines in eukaryotes, cytosine DNA methylation (5mC) has been the focus of most studies so far. In mammals, cytosine methylation is mainly found in "CpGs" (cytosine followed by guanine; here abbreviated CG), while non-CpG methylation (CHG or CHH, where H is any nucleotide other than G) is commonly detected in plants and fungi [3,4]. Various DNA methyltransferases (DNMTs) are involved in the establishment and maintenance of DNA methylation but the distribution and number of enzymes involved is highly variable in different kingdoms [5]. In mammals and plants, enzymes of the DNMT1/MET1 class are maintenance methyltransferases that detect hemi-methylated DNA sequences, for example after replication [6–8]. *De novo* methyltransferases, like DNMT3a and DNMT3b in mammals [9] and DRM in plants [10] act on sequences that are free of methylation, presumably by recognition of specific motifs or patterns [9,11]. Although DNMTs are often classified as maintenance or *de novo* enzymes their function is not necessarily limited to one or the other [12,13].

In fungi, four classes of DNMTs have been identified. Basidiomycetes have DNMT1 homologs that appear to be classical maintenance DNMTs [4,14]. In the ascomycete *Neurospora crassa,* DNA methylation is mediated by a single enzyme, DIM-2 [15]. While the conserved DIM2 class of enzymes shows limited sequence similarity to DNMT1/MET1 maintenance DNMTs, it is a class specific to fungi [16]. Other fungal proteins resembling DNMT1 include *Ascobolus immersus* Masc1 and *N. crassa* RID [17,18], involved in "Methylation Induced Premeiotically" (MIP) or "Repeat-Induced Point mutation" (RIP), respectively [17,19]. DNMT5 enzymes constitute a more recently discovered class of maintenance DNMTs in fungi [20,21]. So far, the presence of 5mC in fungi has been mainly associated with repetitive DNA suggesting a role in genome defense by silencing of transposable elements (TEs). There is little or no evidence that 5mC is also found in coding sequences to influence gene expression [22], although there are examples of promoter methylation [23,24].

A previous study demonstrated amplification of *dim2*, a gene encoding the homolog of *N. crassa* DIM-2, and inactivation by RIP in the genome of the plant pathogenic fungus *Zymoseptoria tritici* [25,26]. For example, the genome of the reference isolate IPO323 carries 23 complete or partial, nonfunctional copies of *dim2*; all alleles show signatures of RIP, namely numerous C:G to T:A transition mutations. Consequently, 5mC was not detected by mass spectrometry in IPO323 [25,26]. However, the amplification of *dim2* must have occurred recently as two closely related sister species of *Z. tritici*, *Zymoseptoria ardabiliae* and *Zymoseptoria pseudotritici* were shown to carry a single intact *dim2* gene and have 5mC [25].

Population genomic analyses have revealed high levels of genetic variation within and between populations of *Z. tritici* [27–29]. This variation is generated by high mutation and recombination rates and by extensive gene flow. Notably, a dynamic landscape of transposable elements in this fungus has been associated with rapid evolution, not only in *Z. tritici*, but also in sister species [30,31]. Moreover, a recent study demonstrated a pervasive effect of recurrent introgression between closely related species

99 of *Zymoseptoria* [32]. These interspecific hybridization events are evident from the presence of highly
100 diverged alleles that are maintained over evolutionary time within species.
101 By genome analyses of multiple *Z. tritici* isolates from the center of origin of the pathogen, the Middle
102 East, we discovered several *Z. tritici* isolates with an intact *dim2* gene. Our findings suggest that the
103 loss of *de novo* 5mC not only occurred very recently but is an ongoing process and polymorphic trait in
104 *Z. tritici*. Here, we address the evolution and function of *dim2* in the *Zymoseptoria* species complex. We
105 show that the presence of an intact and functional *dim2* in some *Z. tritici* isolates corresponds to
106 widespread 5mC in TEs. Integration of a wild-type, intact *dim2* allele into a *dim2*-deficient background
107 restores methylation of previously non-methylated regions. Using comparative genomics and
108 experimental evolution we show that loss of *dim2* and thus 5mC affects nucleotide composition of TEs
109 by influencing mutation rates at CA sites.

Results

The *dim2* DNA methyltransferase gene is functional in several *Z. tritici* isolates

Based on our identification of a non-truncated *dim2* gene in an Iranian *Z. tritici* isolate, Zt10, we set out to investigate its recent evolution in the *Zymoseptoria* species complex in a much larger collection of genome sequences than previously [25] available. We used BLAST to search for the sequence of *dim2* in 22 high-quality assemblies obtained by SMRT sequencing of *Z. tritici* (Fig 1) [33–36], as well as 17 genomes of *Z. ardabiliae*, and nine genomes of *Z. brevis* (S1 Table), both closely related sister species of *Z. tritici* and considered to be endemic to Iran. We detected a single *dim2* homolog in each of the *Z. ardabiliae* and *Z. brevis* genomes but found multiple mutated and non-functional copies of *dim2* in 17 out of 22 *Z. tritici* genomes (Fig 1). Five *Z. tritici* isolates contained an intact, non-mutated copy of *dim2* in addition to multiple mutated, non-functional copies, except for isolate Zt469, which contained one functional *dim2* gene and no additional copies. We considered *dim2* genes intact and functional when they did not contain pre-mature stop codons or frameshift mutations. Non-functional copies contained numerous mutations including pre-mature stop codons.

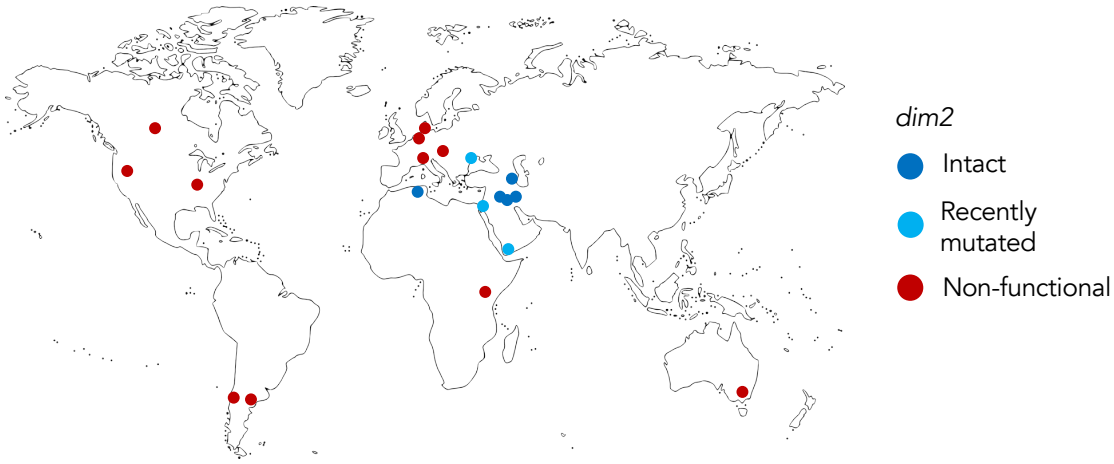

Isolate	Origin	Year	Host	*dim2*
Zt469	Iran	2018	*Aegilops sp.*	+
Zt10	Iran	2001	*Triticum aestivum*	+
Zt289	Iran	2001	*Triticum aestivum*	+
Zt11	Iran	2001	*Triticum aestivum*	+
TN09	Tunisia	2008	*Triticum turgidum subsp. durum*	+
YEQ92	Yemen	1991	*Triticum aestivum*	-*
ISY92	Israel	1992	*Triticum aestivum*	-*
UR95	Ukraine	1995	*Triticum aestivum*	-*
KE94	Kenia	1994	*Triticum aestivum*	-
CRI10	Czech Republic	2010	*Triticum aestivum*	-
Zt05	Denmark	2009	*Triticum aestivum*	-
Zt09	Netherlands	1984	*Triticum aestivum*	-
Zt1A5	Switzerland	1999	*Triticum aestivum*	-
Zt1E4	Switzerland	1999	*Triticum aestivum*	-
Zt3D1	Switzerland	1999	*Triticum aestivum*	-
Zt3D7	Switzerland	1999	*Triticum aestivum*	-
OregS90	USA	1990	*Triticum aestivum*	-
I93	USA	1993	*Triticum aestivum*	-
CNR93	Canada	1992	*Triticum aestivum*	-
Arg00	Argentina	2000	*Triticum turgidum subsp. durum*	-
CH95	Chile	1994	*Triticum aestivum*	-
Aus01	Australia	2001	*Triticum aestivum*	-

Fig 1. Overview of sampling location, year, host plant, and presence of a functional *dim2* DNA methyltransferase gene of *Z. tritici* isolates analyzed in this study.
Aegilops sp., wild grass in Triticeae; *Triticum aestivum*, bread wheat; *T. turgidum durum*, Durum wheat. *non-functional, recently mutated native *dim2* gene

Zt469 was isolated from *Aegilops sp.*, all other isolates were collected from wheat. Four of those five isolates with intact *dim2* are from Iran (Zt10, Zt11, Zt289, Zt469) [33,37], and one is from Tunisia (TN09, collected from durum wheat) [33]. We further tested whether presence of a non-mutated *dim2* allele is commonly found among Iranian isolates. Twelve additional isolates from Iran (S1 Table) were assayed by PCR and Sanger sequencing and in all cases, we confirmed presence of an intact *dim2* allele. A region of chromosome 6 of IPO323 had been previously identified as the native *dim2* locus; all additional, non-functional copies are located in subtelomeric regions embedded in repetitive DNA [25]. Consistent with this idea, we found that all non-mutated *dim2* genes were located at the predicted native locus on chromosome 6 (Fig 2A, S2 Table).

Analyses of *Z. tritici dim2* alleles reveals multiple cycles of recombination and inactivation

Previously, gene amplification of the native *dim2* allele, followed by RIP had been suggested as the most likely cause for the apparent lack of 5mC in the *Z. tritici* IPO323 genome [25,26]. We here conducted a detailed analysis of mutations within native and non-native *dim2* genes in the *Z. tritici* genomes and found some unexpected patterns.

Indeed, as previously reported, non-functional copies of *dim2* contain numerous transition mutations as a consequence of RIP, thus to compare sequences of native and additional (non-native) copies we "deRIPed" mutant copies by reverting C→T and G→A transitions using the functional *dim2* from Zt469 as reference, because it likely represents one ancestral allele. We found that all non-native alleles share a specific pattern of transition and, surprisingly, transversion mutations in the DNA methyltransferase domain that are not found in the vast majority of native *dim2* genes (Figs 2A, S1A and S2). Transversions are not a consequence of RIP [38,39], thus a mixture of transitions, transversions, and deletions suggests that *dim2* was mutated not simply as a result of amplification of the native gene followed by widespread RIP, as originally proposed [25]. Rather, integration of a different *dim2* allele (hereafter called transversion allele) of unknown origin into subtelomeric regions is likely to have resulted in subsequent gene amplification, RIP and presence of multiple non-functional, non-native *dim2* copies. In support of this hypothesis, we found that the flanking regions of the additional, but not the native, copies share homology and are annotated as retrotransposons, suggesting that integration and amplification of non-native copies may have been TE-mediated.

While this idea explains events at subtelomeric integrations sites, we also identified two isolates in which the native *dim2* gene on chromosome 6 shares the specific transversion mutations in the DNA methyltransferase domain, OregS90 and CRI10 (from the USA and Czech Republic, respectively) (Fig 2A). The native OregS90 *dim2* is truncated and surrounded by TEs and the native *dim2* of CRI10 lacks mutations in the 3' region that are present in all additional, but not native, copies.

Five native *dim2* genes have a shared deletion in the 5' region that is not found in any of the additional copies. Given the previously identified signatures of introgression in *Z. tritici* genomes we

166 consider that these different *dim2* alleles at the native locus may reflect separate integration events that
167 have been directed by sequence identity. In summary, our analyses revealed that gene amplification
168 followed by RIP alone is insufficient to explain the distribution of variant *dim2* alleles in *Z. tritici* isolates.
169
170 To further investigate the evolutionary history of *dim2* in *Z. tritici* isolates, we compared the
171 sequence identity of the non-mutated *dim2* gene from Zt469 to all other, native and additional, copies
172 of *dim2* in the 22 *Z. tritici* genomes (Fig 2B). Gene amplification followed by RIP predicts that by
173 accumulating transition mutations all copies should become quite similar to each other; RIP becomes
174 less efficient or stops when sequence identity between alleles drops to ~80% [38]. Instead, our analyses
175 revealed that 18/21 isolates showed two distinct patterns, the first matching the prediction because
176 isolates lacking functional *dim2* showed higher levels of DNA sequence identities (85-95%) between
177 native and additional alleles (Fig 2B, S2 Table; red, "non-functional", pattern 1). Here, all copies have
178 suffered repeated RIP cycles, and all copies are non-functional. When, however, an intact, native *dim2*
179 allele is present (pattern 2), the additional copies show lower DNA sequence identities (84-88%) while
180 the functional alleles are almost identical (>96%) to the Zt469 allele (Fig 2B, S2 Table; dark blue, "intact";
181 Zt10, Zt289, Zt11, TN09). This second pattern was unexpected; the most parsimonious explanation is
182 replacement of non-functional alleles at the native locus with novel *dim2* alleles, perhaps by
183 recombination with wild grass infecting isolates, such as Zt469.
184 We discerned a third group of three isolates, which suggests that repeated cycles of transposon- or
185 recombination-mediated amplification of *dim2* alleles are still ongoing (Fig 2B, S2 Table; light blue,
186 "recently inactivated"; YEQ92, ISY92, UR95). YEQ92 and ISY92 contain non-functional *dim2* alleles at
187 the native locus that are still similar (96 and 92%, respectively) to the functional *dim2*, suggesting a more
188 recent inactivation of *dim2* in these isolates. All additional, subtelomeric copies have low sequence
189 identities as in the second pattern described above. UR95 has two recently mutated *dim2* alleles, one
190 at the native locus (Zt469 allele) and one in the subtelomeric region on chromosome 8 (transversion
191 allele); both are non-functional alleles but contain relatively few mutations and are still similar to the
192 functional *dim2* allele (>90%) suggesting recent integration and inactivation. In summary, our findings
193 suggest that there are multiple functional alleles of *dim2* at the native locus present in the *Z. tritici*
194 population. One group of alleles is derived from the Zt469 allele, a second group contains the
195 "fingerprint" of the transversion allele when compared to the Zt469 allele.

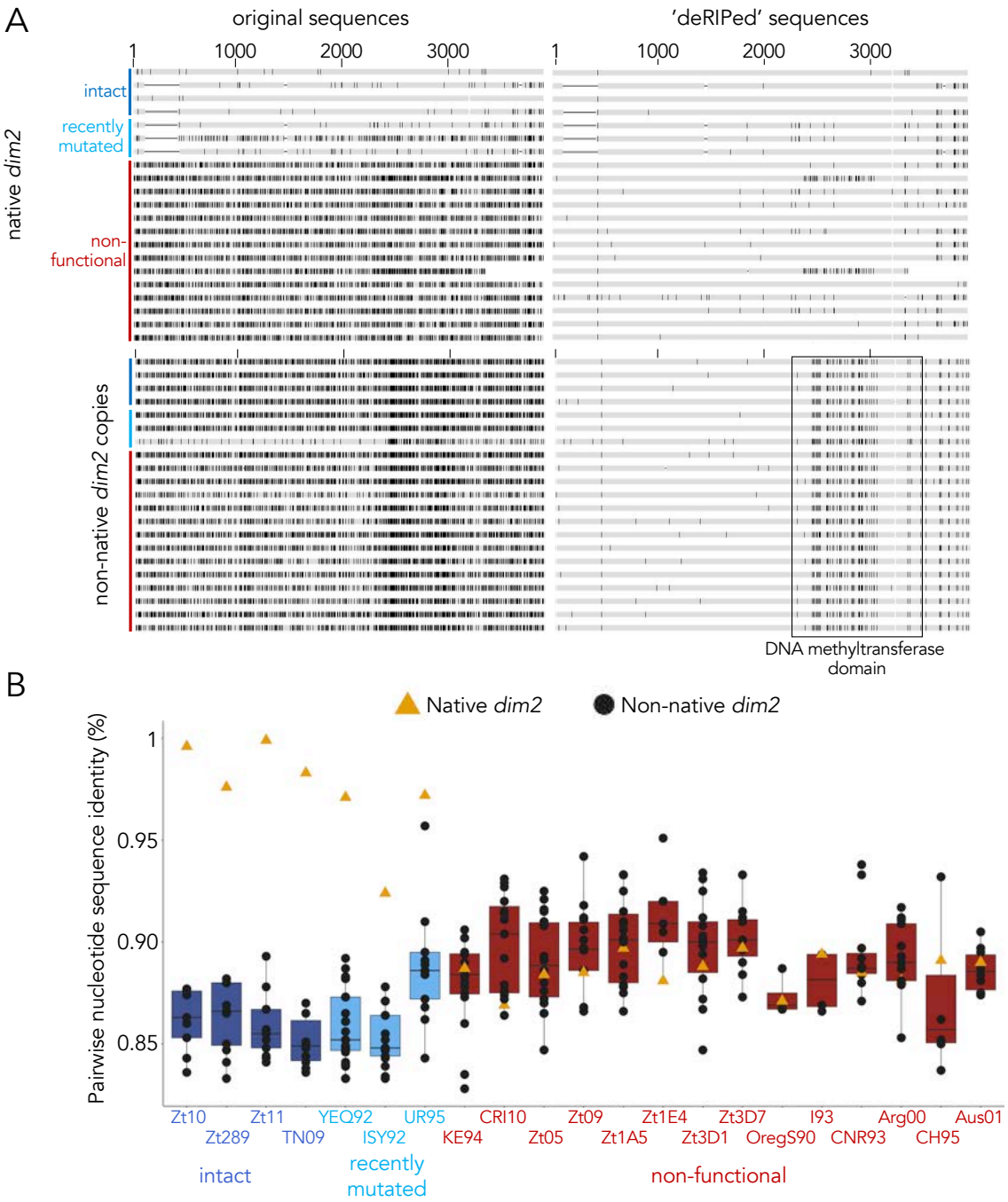

Fig 2. Sequence comparisons of *dim2* alleles in *Z. tritici* isolates.
A) Mutations of *dim2* in original and 'deRIPed' alleles identified by alignment to the functional allele of Zt469. Shown are all native alleles (located on chromosome 6) and one representative non-native, additional copy per isolate. Native alleles (functional and non-functional) lack mutations in the DNA methyltransferase domain that are present in all non-native alleles (black box), except for isolates OregS90 and CRI10. **B)** Pairwise sequence comparison of the native, intact *dim2* allele from Zt469 with all full-length native and additional *dim2* sequences (see S2 Table). No additional *dim2* copies were detected in the genome of Zt469 (from *Aegilops sp.*) whereas all other isolates (from *Triticum* spp.) have additional copies of *dim2*. Non-native, additional copies (black dots) in the isolates with functional or recently mutated *dim2* (except for UR95) showed higher sequence diversity compared to those with inactivated *dim2*, where alleles at the native locus (yellow triangle) are amongst the more diverged copies. This supports the idea that this is the ancestral, now heavily mutated allele of *dim2*. Alleles or isolates are arranged in the same order in panels A (top to bottom) and B (left to right).

210 **Integration of an intact *dim2* allele at the native locus restores 5mC in Zt09**

211 To assess the role of *dim2* in DNA methylation we generated mutants in which we either restored or
212 deleted *dim2*. We integrated the functional *dim2* gene of the Iranian Zt10 isolate into the native *dim2*
213 locus of Zt09 (derived from reference isolate IPO323) by selecting for hygromycin resistance, conferred
214 by the *hph* gene, generating the strain Zt09::*dim2*. In Zt10, we replaced the functional *dim2* gene with
215 *hph*, generating the strain Zt10Δ*dim2*. Integration or deletion of the *dim2* alleles were verified by
216 Southern analyses (S3 Fig). To test whether *dim2* affects growth or infection, we compared the mutant
217 and respective wild-type strains under different *in vitro* conditions as well as during host infection. We
218 did not detect any differences between wild-type and mutant strains *in vitro* (S4 Fig) but integration of
219 the functional *dim2* in Zt09 significantly reduced necrosis and asexual fruiting body formation (measured
220 as number of asexual fruiting bodies, pycnidia, per leaf area) *in planta* (S5 Fig). We therefore conclude
221 that presence of *dim2* is dispensable under the tested *in vitro* conditions but that re-integration of *dim2*
222 into the Zt09 background decreases virulence *in planta*.

223 To validate the presence of 5mC and to compare patterns between isolates and mutants, we
224 performed whole-genome bisulfite sequencing (WGBS). We sequenced three replicates of each wild-
225 type isolate (Zt09 and Zt10) and mutant strain (Zt09::*dim2* and Zt10Δ*dim2*). As a control for the bisulfite
226 conversion rate, we added Lambda DNA to each sample; based on this, the bisulfite conversion rate
227 was >99.5%. To confirm the WGBS sequencing results, we performed an additional independent
228 bisulfite conversion, amplified target regions by PCR, cloned and sequenced the fragments, and we
229 performed Southern blot analyses using 5mC-sensitive and -insensitive restriction enzymes (S6 Fig).

230 We detected high numbers of methylated cytosines in isolates with functional *dim2* alleles, i.e., the
231 wild-type Iranian isolate Zt10 and Zt09::*dim2*. Surprisingly, we also detected low levels of 5mC in the
232 absence of *dim2*, i.e., in Zt10Δ*dim2* and Zt09, which had been missed by the mass spectrometry in
233 earlier studies [25]. While on average ~300,000 sites in Zt10 and ~400,000 sites in Zt09::*dim2* showed
234 5mC in the presence of *dim2*, only ~12,000 (Zt09) and ~40,000 (Zt10Δ*dim2*) 5mC sites were found when
235 *dim2* was absent (Fig 3A). In all strains, 5mC was restricted to previously annotated TEs and adjacent
236 non-coding regions (Fig 3A). We did not find evidence for gene body or promoter methylation, except
237 for few TE-derived genes. By correlating the 5mC data with previously published histone methylation
238 maps [40] we found that 5mC co-localizes with H3K9me3 marks (Fig 3B). This finding is consistent with
239 observations in *N. crassa*, *C. neoformans*, and *A. thaliana* [21,41–44].

240 We next analyzed the specific context of DNA methylation. In strains without functional *dim2*, we
241 found 5mC exclusively in CG contexts (genome wide ~0.2% in Zt09 and ~1% in Zt10Δ*dim2*; percentage
242 based on all Cs in the genome*)*. In the presence of *dim2*, cytosines in CG as well as CHG and CHH
243 contexts were methylated. Genome-wide, ~5 or 6% of CGs and <1% of CHGs or CHHs were methylated
244 in Zt10 or Zt09::*dim2*, respectively (Fig 3C). In sequences annotated as TEs, however, up to 60% of all
245 CGs were methylated (Fig 3D). Methylation of CGs occurred most frequently (~43%, ~61%), but we
246 also detected methylation at CAs (~10%, ~22%), and to lesser extent at CCs (~3%, ~8%). At CTs, there
247 was hardly any detectable methylation (<0.01%; Figs 3D, S7) in Zt10 or Zt09::*dim2*, respectively. This
248 was surprising, as CTs are the most abundant CH dinucleotides in TEs while CAs are the least abundant

249 sites in genomes of both Zt09 and Zt10 (S3 Table). This suggests a strong site-specific preference of
250 Dim2 for CAs but not CTs in *Z. tritici*.

251 Upon integrating of a functional *dim2* allele in Zt09 we found that overall 5mC levels are higher when
252 compared to Zt10 (compare Fig 3C, left- and right-most panels), and CG methylation levels in Zt10Δ*dim2*
253 were higher compared to Zt09 (compare Fig 3C, two middle panels). These findings suggest that 5mC
254 levels can decrease significantly over relatively short evolutionary time spans even if a *de novo* DNA
255 methyltransferase is present.

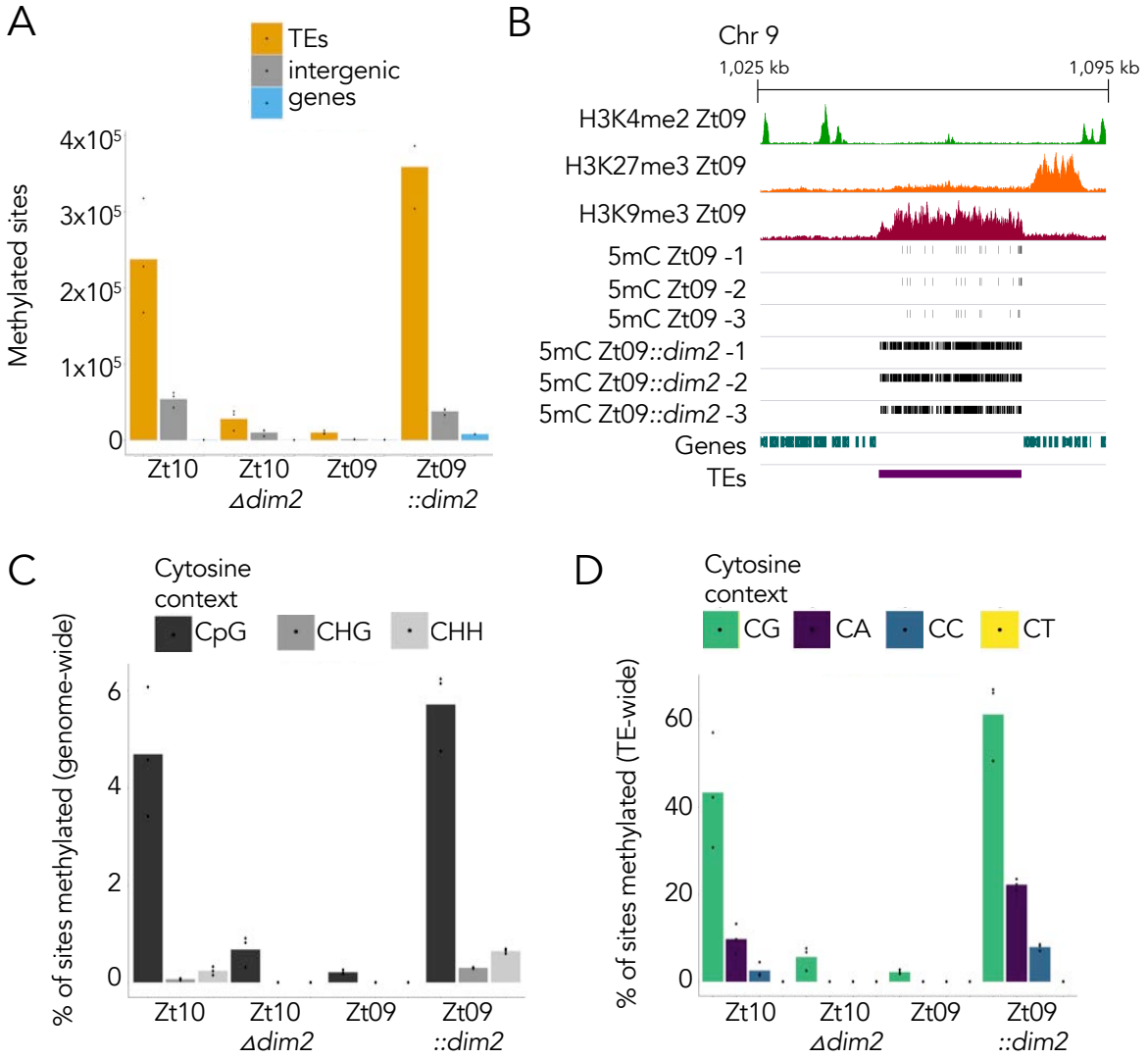

256

257 **Fig 3. Localization and site preferences of cytosine methylation in *Z. tritici* genomes in presence**
258 **and absence of *dim2*. A)** Number of 5mC methylated sites detected by whole genome bisulfite
259 sequencing (WGBS) in TEs, intergenic regions, or genes. The vast majority of methylated sites is
260 localized in TEs followed by intergenic regions and TE-derived genes. **B)** 5mC co-localizes with
261 H3K9me3 and TEs in Zt09. Shown are ChIP-seq tracks for H3K4me2, H3K27me3 and H3K9me3 [40],
262 and 5mC sites detected in a representative region on chromosome 9 in the genomes of Zt09 and
263 Zt09::*dim2* (three replicates). **C)** Genome-wide 5mC levels in the different isolates and respective
264 mutants. 5mC levels are higher in the presence of *dim2*, and *dim2* is required for all non-CG methylation.
265 **D)** 5mC levels and site preferences in TEs. CG sites are preferred, followed by CA, and CC. 5mC is
266 almost completely absent from CTs.

267 **DNA methylation can be maintained in absence of *dim2***

268 We next asked how 5mC can persist in the genome of *Z. tritici* in the absence of a functional *dim2* gene.
269 The presence of CG methylation in isolates without *dim2* suggested the presence of an additional
270 DNMT. Thus, we searched for putative DNMT coding regions in the genomes of *Z. tritici*, *Z. ardabiliae*,
271 and *Z. brevis* with the conserved DNMT domain of Dim2 as query in a BLASTp search. In all genomes,
272 we found two additional predicted DNMTs (S8 Fig). One is similar to Dnmt5 of *Cryptococcus neoformans*
273 [20] *(dnmt5*, Zt_chr6_00685), the other is a homolog of *N. crassa* RID [17] (*rid*, Zt_chr5_00047; manually
274 corrected gene annotation) [45]. Genes for Dnmt5 and Rid are present in all *Zymoseptoria* spp. genomes
275 we analyzed. The *dnmt5* alleles are highly conserved and show very little inter- or intraspecies diversity
276 (S1B Fig). In contrast, *rid* shows an exceptionally high inter- and intraspecies diversity with three highly
277 distinct alleles present in *Zymoseptoria* spp. (S1C Fig). This diversity may stem from introgression
278 events between *Zymoseptoria* species as recently described for highly variable regions in the genome
279 of *Z. tritici* [32]. However, presence of the different *rid* alleles does not correlate with presence of a
280 functional *dim2* gene in *Z. tritici*.

281 Masc1 and RID are involved in genome defense during pre-meiosis [17,18]. Although Masc1 is
282 presumed to be a *de novo* DNMT acting during the sexual cycle of *Ascobolus immersus*, there are still
283 no enzyme activity data available for either Masc1 or RID. In contrast, Dnmt5 has been characterized
284 as a 5mCG maintenance DNMT in *C. neoformans* [20,21] and is thus the most likely candidate for
285 maintenance of 5mC at CG sites that we observed here. Further studies will address the role of *dnmt5*
286 in maintenance and impact on 5mC in *Z. tritici*.

287

288 **Presence of *dim2* impacts nucleotide composition and activity of TEs**

289 DNA cytosine methylation is correlated with increased C→T mutation rates [46,47]. In *Z. tritici*, and most
290 other fungi [22], 5mC is enriched in TE sequences. To evaluate whether the presence of *dim2* impacts
291 sequence composition of TEs, we analyzed TE sequences in isolates with and without a functional *dim2*
292 gene. Therefore, we extracted TE sequences, calculated dinucleotide frequencies relative to the TE
293 content for each genome (S3 Table), and visualized the difference in frequencies by correspondence
294 analysis. Isolates lacking functional *dim2* have more CA/TG sites within TEs compared to isolates with
295 functional *dim2* (Fig 4A, B). Conversely, isolates with functional *dim2* contain more TA sites in TEs (Fig
296 4A, B). Two isolates with recently inactivated *dim2*, ISY92 and YEQ92, show the same pattern as
297 isolates with functional *dim2* but UR95, with two more recently inactivated copies, groups with isolates
298 lacking functional *dim2*. CA/TG sites are the least frequent sites in TEs, while TA sites are the most
299 abundant. We observed the same pattern (i.e., increased number of TA sites), when we included the
300 sister species *Z. ardabiliae* (Za17) and *Z. brevis* (Zb87), and the more distantly related barley pathogen,
301 *Z. passerinii* (Zpa63), all of which contain a single, functional *dim2* (Fig 4B; S3 Table). This pattern is
302 only detectable in TEs, not in the rest of the genome (S3 Table).

303 Accelerated mutation rates in TEs may impact TE activity, so we next determined the TE content of
304 the various *Z. tritici* isolates and compared it to that observed in other *Zymoseptoria* species (Fig 4C).
305 Isolates with functional *dim2* had slightly lower TE content than those lacking *dim2* (~16.2% *vs.* ~18.7%;

306 Fig 4C) but TE content in other *Zymoseptoria* species, all with functional *dim2*, was higher than in many
307 *Z. tritici* strains. Thus, there is no simple or clear correlation between TE content and *de novo* 5mC
308 activity. GC content of TEs, however, is considerably lower in isolates with functional *dim2* and two
309 isolates with recently mutated *dim2*, ISY92 and YEQ92, further indicating that Dim2 impacts nucleotide
310 composition (Fig 4C).

311 The TE content of a genome does not necessarily reflect the activity of TEs, as these sequences
312 may be relics, i.e., mutated and thus inactivated TEs. We therefore assessed whether TEs in Zt09 and
313 Zt10 contained annotated, transposon-related genes as a putative indicator for the presence of active
314 TEs. In Zt09, 56 genes completely overlap (>90% of the sequence) with annotated TEs. Among those,
315 we identified 30 transposon- or virus-related genes encoding for endonucleases, transposases,
316 ribonucleases, and reverse transcriptases, or genes encoding virus-related domains (S4 Table). In
317 contrast, we did not detect any fungal genes overlapping TEs in Zt10. We did find homologs of some of
318 the transposon-associated genes of Zt09 in the genome of Zt10, but they all contained numerous
319 transitions resulting in mis- and nonsense mutations. This indicates that Zt09 contains active TEs
320 whereas homologous elements are inactivated in Zt10.

321 Lastly, we compared the expression of TEs in Zt09 and Zt10 during the time course of infection by
322 analyzing previously published RNA-seq data [36]. We computed transcripts per million (TPM)
323 originating from TEs in both the biotrophic and necrotrophic phases of infection and considered a TE
324 expressed when TPM was > 0. While ~21% of TEs produced RNA in Zt10, ~35% of TEs were
325 transcribed in Zt09 (Fig 4D) indicating that silencing of TE loci is less pronounced in Zt09 where *dim2* is
326 non-functional.

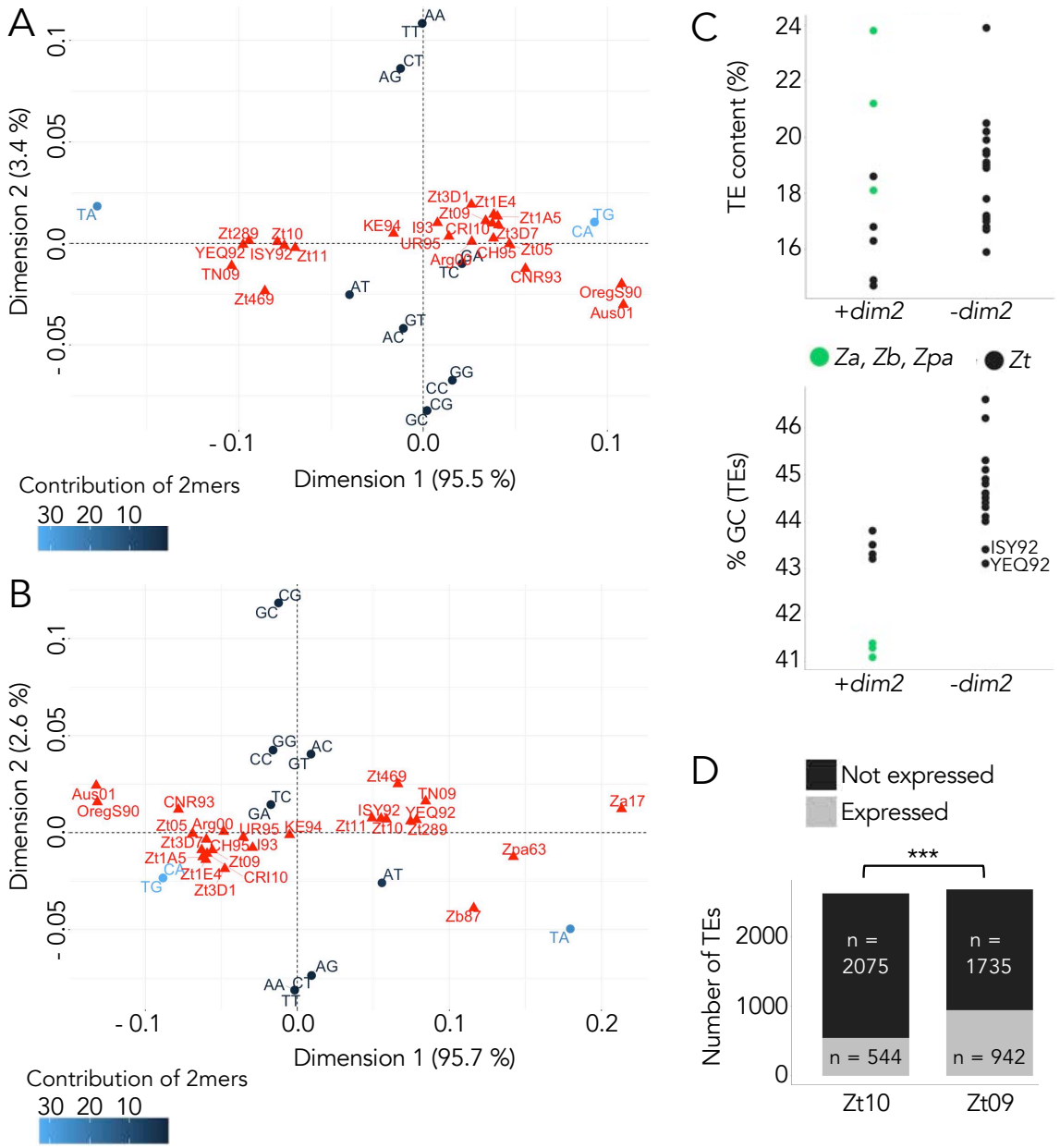

Fig 4. Impact of Dim2 on nucleotide composition and TE activity. A) and **B)** Correspondence analyses showing differences in dinucleotide (2mer) frequencies in TEs of different *Z. tritici* isolates **(A)** and other members of the *Zymoseptoria* species complex **(B)**. TA and CA/TG dinucleotide frequencies have the highest impact on the observed differences between isolates and species, indicated by their relative positions on the dimension 1 *versus* dimension 2 plot. Isolates (even from different species) containing an intact *dim2* (Zt10, Zt289, Zt11, Zt469, TN09, Zb87, Za17, Zpa63) and recently mutated *dim2* (ISY92 and YEQ92) have higher TA content and cluster together, while isolates without functional *dim2* have higher CA/TG frequencies in TE sequences. **C)** Comparison of TE and GC content between different *Z. tritici* isolates and *Zymoseptoria* species with and without functional *dim2*. **D)** Number of expressed TEs during the time course of wheat infection is significantly higher in *Z. tritici* isolate Zt09 (non-functional *dim2*) compared to Zt10 (intact *dim2*) (Fisher's Exact Test for Count Data, *p*-value < 2.2 x 10^{-16}).

341 **Dim2 promotes C→T transitions at CAs during mitosis**

342 The difference between CA/TG and TA site abundance in genomes with and without functional *dim2*
343 suggests that the mutation rate, specifically for C→T transitions, is affected by the presence of 5mC. To
344 address whether Dim2 plays a role in promoting these mutations, we conducted a one-year evolution
345 experiment that included the Iranian isolate Zt10 (functional *dim2*) and the reference isolate IPO323
346 (non-functional *dim2*, isolate Zt09 is a derivate of IPO323). This was a mutation accumulation
347 experiment without competition or selection on cells that were dividing by mitosis only. Each ancestral
348 isolate was propagated as 40 independent replicates. After 52 weeks (corresponding to ~1,000 mitotic
349 cell divisions) the genomes of the 40 evolved replicate strains per isolate and the progenitor isolates
350 were sequenced to map SNPs. We found that the mutation rate in Zt10 was more than tenfold higher
351 than in IPO323, on average ~170 *vs.* ~13 mutations per replicate (Fig 5A, S5 Table). The vast majority
352 of mutations in Zt10 (> 95%) occurred in 5mC regions (S6 Table) and > 95% of all mutations were C→T
353 transitions, while only ~32% of all mutations in IPO323 were C→T transitions. In Zt10, > 98% of the
354 C→T transitions occurred at CAs (*vs.* ~21% in IPO323) (Fig 5B). This was a surprise, because the
355 majority of methylated sites are at CGs. Our findings suggest the presence of a *dim2*-dependent
356 mechanism that specifically targets and mutates CA/TG but not CGs in sequence repeats during mitosis.
357 Such a mutator resembles the hitherto undescribed but much looked-for mitotic version of RIP.

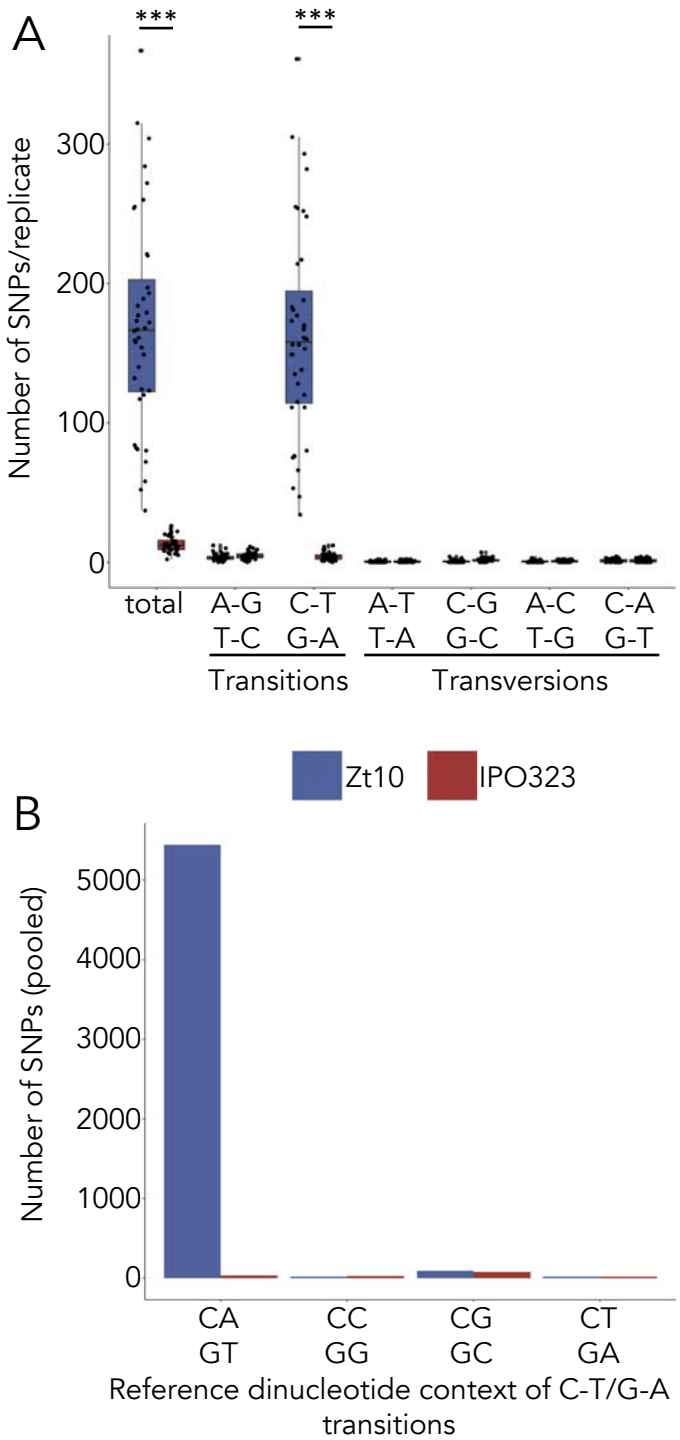

Fig 5. Number and site preferences of SNPs in isolates with functional (Zt10) and non-functional (IPO323*) *dim2* after one year of mitotic growth. A) Detected number of SNPs in the 40 replicates of each isolate. The number of SNPs in Zt10 replicates is significantly higher compared to IPO323 (Wilcoxon rank sum test, ****p*-value < 0.001). The vast majority of mutations are C to T transitions. **B)** Sequence context of the mutations in the two tested isolates. The SNPs of all replicates were pooled for this analysis. C→T transitions are predominantly found in a CA context resulting in CA to TA (or GT to TA) mutations. CG sites, although preferentially methylated, are not mutated at high rates.
*Isolate Zt09 is a derivate of IPO323.

385 **Discussion**

386 Our study of the DNA methyltransferase *dim2* in the fungus *Z. tritici* reveals an exceptional extent of
387 intra species polymorphism that has functional and genetic implications. Although it has been reported
388 that 5mC is absent in *Z. tritici* [25], we found that some isolates contain a functional Dim2 *de novo* 5mC
389 methyltransferase. We show that loss of most 5mC is quite recent; we found that 5mC is not completely
390 absent in *Z. tritici*, even when there is no functional Dim2; and we identified a Dim2-dependent mutator
391 phenomenon. The majority of isolates in which we identified non-mutated *dim2* genes originated in Iran,
392 previously shown to be the center of origin of *Z. tritici* [37]. The closely related sister species *Z. ardabiliae*
393 and *Z. brevis* were collected in Iran as well and are so far considered to be endemic to this region
394 [48,49]. We found only one *Z. tritici* isolate (Zt469) that did not carry any additional *dim2* copies. This
395 isolate was collected from *Aegilops* sp., also in Iran. We propose that the original state of the native
396 *dim2* locus has been maintained in the two sister species and *Z. tritici* isolates collected from wild
397 grasses. Even functional *dim2* alleles show sequence polymorphisms, i.e., transitions and mid-size in-
398 frame deletions, respectively. Thus, all available data suggest that *dim2* gene amplification,
399 recombination events, and RIP have been specific to wheat-infecting *Z. tritici* isolates.

400 Here, we disproved a previous hypothesis, suggesting that the mutated *dim2* copies in IPO323 and
401 similar strains arose by gene duplications of the native *dim2* followed by transposon-mediated
402 movement to subtelomeric regions and RIP [25]. Instead, DNA sequences of the non-functional
403 subtelomeric *dim2* copies show patterns of increased transversion mutations specifically in the DNMT
404 catalytic domain of the gene. This pattern is not an expected outcome of RIP. Instead we consider
405 interspecific hybridization and introgression between distinct lineages with different *dim2* alleles. Our
406 findings suggest that there are at least two groups of functional *dim2* alleles at the native locus in the
407 extant *Z. tritici* population. One group is derived from or similar to the Zt469 allele, a second group of
408 alleles is enriched with "transversions" when compared to the Zt469 allele. Two strains, OregS90 and
409 CRI10, had non-functional "transversion alleles" at the native locus and we speculate that both may be
410 derived by secondary integration events. Isolate UR95 contains numerous non-functional copies but
411 also two more recently mutated alleles, one Zt469-type and one transversion allele, both non-functional.
412 This indicates that intact and functional copies of both types of alleles are still present in *Zymoseptoria*
413 populations. The current set of genomes did not reveal a functional "transversion allele" at the native
414 locus or subtelomeric region, but we identified a putative functional copy in WAI329, an Australian
415 Illumina-sequenced isolate [50]. A likely scenario for repeated invasion and inactivation cycles predicts
416 that some wild grass infecting isolates carried "transversion alleles" that were not mutated. Gene
417 amplification or TE-mediated recombination coupled to RIP resulted in numerous non-functional alleles.
418 Our data suggest recombination between isolates with *dim2* non-native transversion alleles, which may
419 have induced RIP in the native *dim2* allele because of high sequence similarity outside of the DNMT
420 catalytic domain, thus resulting in non-functional *dim2* alleles only, and therefore absence of *de novo*
421 DNMT activity. This is consistent with the previously reported signatures of re-current introgression in
422 *Z. tritici* [32]. Further analyses of diverse *Z. tritici* isolates from different hosts and geographical locations

423 (*T. aestivum*, *Triticum durum*, or *Aegilops* sp.) are needed to track the evolutionary history of the *dim2*
424 gene in the *Zymoseptoria* species complex.
425 The previous study on *dim2* suggested absence of 5mC based on liquid chromatography coupled
426 with electrospray ionization tandem mass spectrometry (ESI–MS/MS) [25]. This finding is consistent
427 with the low levels of methylation we discovered in strains lacking Dim2 activity. Based on recent results
428 obtained in studies with *Cryptococcus* we hypothesize that this low level of 5mC has been maintained
429 by the single homologue of Dnmt5 [20,21] after the loss of Dim2. This DNMT acts as a maintenance
430 DNMT but does not catalyze *de novo* DNA methylation [21]. In the absence of a *de novo* DNMT, DNA
431 methylation is likely to decrease over time as any loss of 5mC cannot be restored. This idea is supported
432 by our finding that 5mC levels are higher upon deletion of *dim2* (Zt10Δ*dim2*) compared to Zt09, where
433 *dim2* was likely inactivated thousands of generations ago.
434 Sequence repeats are the predominant targets of DNA methylation in fungi [15,22,51,52], and 5mC
435 enrichment is correlated with genome defense mechanisms that act to silence transposons [1]. We
436 found that nucleotide composition in TEs differs between isolates and species that have functional or
437 non-functional *dim2* alleles. CA sites, the preferred target sites of Dim2 in addition to CGs, are reduced
438 in frequency when Dim2 is present. TA sites, however, are more frequent when Dim2 is present. This
439 links increased C→T transition frequency to the presence of functional Dim2. Spontaneous deamination
440 of 5mC also yields C→T transitions [47], giving rise to accelerated mutation rates at 5mC sites, a well-
441 known phenomenon [53]. Correlation of decreased C:G to T:G transitions in absence of the DNA
442 methyltransferase *CMT3* was recently shown in plants [54]. However, the observed differences in
443 dinucleotide frequencies in *Zymoseptoria* and the high rate of C→T transitions in the evolution
444 experiment suggest a role of Dim2 and 5mC in the generation of mutations. The mutations occurring
445 throughout the evolution experiment specifically affected CAs but not CGs. If mutations resulted from
446 spontaneous deamination, we would have expected a greater effect on CGs because they have higher
447 5mC levels. Lack of Dim2 resulted in complete loss of 5mC at CAs and therefore reduced CA to TA
448 mutation frequencies. We also did not observe a noticeable difference of CG site abundance between
449 isolates with or without functional Dim2, suggesting that non-CG 5mC (mediated by Dim2) is the main
450 driver of the C→T transitions we observed. This suggests that, although repetitive regions are a shared
451 target for DNMTs in different fungal species, distinct target sites of 5mC may correlate with the sequence
452 composition of repetitive regions and the presence of other proteins involved in the 5mC pathway.
453
454 What is the underlying mechanism for the reduced CA to TA mutation frequency in absence of
455 functional *dim2*? The best-known process causing C→T transitions in fungi is RIP, which occurs during
456 pre-meiosis after fertilization but before karyogamy [38,39]. While RIP depends largely on the presence
457 of the putative DNMT, RID [17], DIM-2 has also been suggested to be involved in RIP in *N. crassa* [19].
458 Thus, we propose that the absence of Dim2 may also play a role in the efficiency and rate of RIP in *Z.*
459 *tritici*. Mechanistic studies are lacking to address this question.
460 There is little precedence for a mutator process that generates CA to TA mutations and acts during
461 vegetative growth in any eukaryote, the type of mutator uncovered by our evolution experiment. In *N.*

462 *crassa*, RIP acts preferentially on CAs [19,39,55], and DIM-2 preferentially methylates CTs [22].
463 Presence of *Z. tritici* Dim2 yields non-CpG 5mC preferentially at CAs and increases C→T mutations.
464 Essentially, the *dim2*-dependent phenomenon described here resembles what is expected for a mitotic
465 version of RIP. We do not know yet whether Dim2 is directly involved in this mechanism and whether
466 Rid may also play a role. However, functional alleles of *rid* are present in all strains we analyzed in the
467 evolution experiment, and in all species examined so far *rid* is expressed solely late during the sexual
468 cycle [17]. Experiments with bacterial DNMTs uncovered inherent mutator activity under appropriate
469 environmental conditions (e.g., low concentrations of the methyl donor, *S*-adenosylmethionine [SAM])
470 or when specific point mutations (e.g., in the SAM-binding motif) where generated [56–61]. Another
471 possible mechanism may involve differences in DNA repair efficiency where CG sites are more
472 efficiently repaired compared to CA sites. Hemi-methylation of mutated CG sites could hereby aid in
473 strand recognition and mismatch repair as suggested in mammalian cells [62]. Our ongoing studies are
474 directed towards uncovering sequence motifs in Dim2 and examining growth conditions that increase
475 or decrease the novel mutator phenotype.
476 Why are presence of widespread 5mC and differences in mutation rates polymorphic traits in this
477 fungal pathogen? In several fungal species, 5mC is completely absent or methylation levels are very
478 low [22,63–65] raising the question about the importance of 5mC in terms of genome defense and
479 evolution. While silencing or inactivation of TEs protects genome integrity and stability, it may limit the
480 adaptive potential in response to changing environmental conditions. Transposon-mediated genome
481 diversity, gene or even chromosome copy number variations are frequently found in fungal pathogens,
482 and they form a crucial aspect of rapid evolution [66–69]. Here we uncovered a system of continuing
483 loss and re-acquisition of the ability to silence or inactivate TEs in the genomes of numerous isolates of
484 an important plant pathogen, *Z. tritici.* Based on currently available data, increased 5mC levels
485 negatively affect virulence on wheat, suggesting that loss of *dim2* is adaptive for survival in agricultural
486 environments. Nevertheless, in the center of origin, functional *dim2* copies are re-acquired, suggesting
487 that 5mC is important under certain environmental conditions. The efficiency and abundance of DNA
488 methylation and mutations may therefore represent an evolutionary trade-off between genome integrity
489 and adaptive potential.

490 ## Materials and Methods

491

492 **Fungal isolates and growth conditions**

493 All *Zymoseptoria* spp. isolates used in this study (Table S1) were cultivated at 18°C in YMS (4 g yeast
494 extract, 4 g malt, 4 g sucrose per 1 L, 20 g agar per L for plates) medium. Cultures for DNA extraction
495 and plant infection experiments were inoculated directly from the -80°C glycerol stocks and grown in
496 liquid YMS medium at 200 rpm for 5 days (DNA extractions) and in pre-cultures (3 days) and main
497 cultures (2 days) for plant infections.

498

499 **SMRT sequencing and assembly of Iranian isolates Zt289 and Zt469**

500 High molecular weight DNA was extracted as previously described [70]. Library preparation and PacBio
501 sequencing was performed at the Max Planck Genome Center in Cologne, Germany
502 (https://mpgc.mpipz.mpg.de/home/) with a Pacific Biosciences Sequel II. One SMRT cell was
503 sequenced per genome. Genome assemblies were performed as described [71]. Genome assembly
504 statistics are summarized in Table S7.

505

506 **Identification of TEs and analysis of TE expression**

507 We annotated transposable elements with the REPET pipeline
508 (https://urgi.versailles.inra.fr/Tools/REPET) [72] as described in [71]. Briefly, we identified repetitive
509 element consensus sequences in each genome using TEdenovo following the developer's
510 recommendations [72]. We used each library of consensus sequences to annotate genomes using
511 TEannot with default parameters. To evaluate TE activity we analyzed expression *in planta* using RNA-
512 seq data of *Z. tritici* isolates Zt10 and Zt09 [36]. First, raw sequencing reads were quality filtered and
513 trimmed using Trimmomatic [73] and mapped to the respective genome using hisat2 [74]. Reads were
514 trimmed using the following parameters: LEADING:30 SLIDINGWINDOW:4:30 AVGQUAL:30
515 MINLEN:50. After mapping, the resulting aligned read files were used to assess read counts for each
516 stage and replicate (with a total of two replicates per stage). The read count table was generated using
517 TEcount function of the TEtranscript pipeline with the following parameter: -mode multi [75]. Briefly,
518 TEtranscript pipeline counts both uniquely and multi-mapped reads mapped to annotated transposons
519 and genes to attribute transcript abundance. A given TE was considered transcribed only if reads
520 mapped all along the element length, in order to avoid redundancy [75]. Levels of expression were
521 calculated using Transcript per Million (TPM) normalization which corresponds to the normalization of
522 read counts with transposon (or gene) length per million. We considered a TE as 'expressed' if TPM >
523 0.

524 **Sequence identification and comparison of DNA methyltransferases**

525 All analyzed genomes and isolates used in this study are listed in Table S1 and originate from the
526 following studies [32,33,77–81,34–37,48,49,71,76]. We identified homologs of *dim2* using the predicted
527 'deRIPed' protein sequence of *Z. tritici* IPO323 [25] as a template. To compare the sequence identity
528 between active and inactive *dim2* copies in the genome, we used *dim2* of isolate Zt469 as a reference
529 and performed pairwise comparisons. To identify additional putative DNA methyltransferases, we used
530 the DNA methyltransferase domain of the Dim2 protein as query. BLAST searches, phylogenetic trees
531 and alignments were performed using Geneious 'Blast', Geneious 'Alignment' and Geneious 'Map to
532 reference' (Geneious version 10.2.4 (http://www.geneious.com, [82]). A distance tree based on the
533 nucleotide sequence of *dim2*, *rid* and *dnmt5* was generated with the following settings: alignment type:
534 global alignment with free end gaps, cost matrix: 65 % similarity, genetic distance: Jukes-Cantor, tree
535 build method: neighbor joining, outgroup: *Zymoseptoria passerinii* (Zpa63).

536

537 **Generation of *dim2* deletion and integration strains**

538 We transformed the *Z. tritici* isolates Zt09 and Zt10 using an *Agrobacterium tumefaciens*-mediated
539 transformation (ATMT) protocol as previously described [83]. Briefly, we created plasmids containing
540 the integration (pES189) or deletion (pES188) constructs using Gibson assembly [84] (S8 Table). Both
541 constructs contained the hygromycin resistance cassette as selection marker. Plasmids were amplified
542 in *E. coli* TOP10 cells and sequenced to confirm correct assembly of the constructs followed by
543 electroporation of *A. tumefaciens* strain AGL1. *Z. tritici* strains were transformed with the respective *A.*
544 *tumefaciens* strains by co-incubation for 3-4 days at 18°C on induction medium. Following co-incubation,
545 the strains were grown on selection medium containing hygromycin to select for integration of the
546 constructs and cefotaxime to eliminate *A. tumefaciens*. Single *Z. tritici* colonies were selected, streaked
547 out twice and the correct integration of the construct was verified by PCR and by Southern blot analyses
548 (S3 Fig).

549

550 **Bisulfite treatment and sequencing**

551 We extracted high molecular weight DNA of three biological replicates of Zt10 and Zt09 and three
552 independent transformants of Zt10Δ*dim2* and Zt09::*dim2* as described previously [70]. Genomic DNA
553 was sent to the Max Planck Genome Centre in Cologne, Germany (https://mpgc.mpipz.mpg.de/home/)
554 for bisulfite treatment and sequencing. Lambda DNA was used as spike-in (~1%) to determine
555 conversion efficiency. Genomic DNA was fragmented with a COVARIS S2 and an Illumina-compatible
556 library was prepared with the NEXTflex Bisulfite Library Prep Kit for Illumina Sequencing (Bioo
557 Scientific/PerkinElmer, Austin, Texas, U.S.A). Bisulfite conversion was performed using the EZ DNA
558 Methylation Gold Kit (Zymo Research, Irvine, CA). Illumina sequencing was performed on a HiSeq3000
559 machine with paired-end 150-nt read mode (S9 Table).

560 To confirm bisulfite sequencing results, we treated genomic DNA of the fungal strains and, as a
561 control for conversion efficiency, the Universal Methylated DNA Standard (Zymo Research, Irvine, CA)
562 (~100 ng) with bisulfite using the EZ DNA Methylation-Lightning Kit (Zymo Research, Irvine, CA)

563 according to manufacturer's instructions. Two representative loci per fungal strain and the human MLH1
564 for the control were amplified by PCR (ZymoTaq PreMix, Zymo Research, Irvine, CA) using specifically
565 designed primers for amplification of the bisulfite-treated DNA (designed using the 'Bisulfite Primer
566 Seeker' (Zymo Research, Irvine, CA), S8 Table). PCR products were cloned using the TOPO TA kit
567 (Thermo Fisher Scientific) and Sanger sequenced (Eurofins Genomics, Ebersberg, Germany). Analysis
568 of sequenced bisulfite-converted DNA sequences was performed using Geneious software version
569 10.2.4 [82].
570
571 **Data analysis of whole genome bisulfite sequencing data**
572 A list of software and input commands used in our analyses is provided in the S1 text.
573 Reads were quality filtered using Trimmomatic [73] and subsequently mapped using Bismark [85].
574 Duplicate reads were removed. Methylated sites were extracted using the
575 bismark_methylation_extractor applying the –no_overlap and CX options. We considered sites
576 methylated, if at least 4 reads and ≥ 50 % of reads supported methylation. We then extracted these sites
577 (see text S1) in CG, CHG or CHH contexts for further analysis. Bedtools [86] was used to correlate
578 methylation and genomics features.
579
580 **Southern blots to detect DNA methylation and confirm *dim2* mutant strains**
581 To detect presence or absence of 5mC, we performed Southern blots according to standard protocols
582 [87]. Genomic DNA was extracted using a standard phenol-chloroform extraction method [88]. The
583 same amount of DNA and enzymes (*Bfu*CI, *Dpn*I, *Dpn*II; 25 units, New England Biolabs, Frankfurt,
584 Germany) was used as input for the different restriction digests to make restriction patterns comparable
585 between enzymes and *Z. tritici* isolates for the detection of DNA methylation. Probes were generated
586 with the PCR DIG labeling Mix (Roche, Mannheim, Germany) following the manufacturer's instructions
587 and chemiluminescent signals were detected using the GelDocTM XR+ system (Bio-Rad, Munich,
588 Germany).

589 **Phenotypic assay *in vitro***

590 Spores were diluted in water (10^7 cells/mL and tenfold dilution series to 1,000 cells/mL) and three μL of
591 the spore suspension dilutions were pipetted on plates and incubated for ten days. To test for responses
592 to different stress conditions *in vitro*, YMS plates containing NaCl (0.5 M and 1 M), sorbitol (1 M and 1.5
593 M), Congo Red (300 μg/mL and 500 μg/mL), H_2O_2 (1.5 mM and 2 mM), methyl methanesulfonate (0.01%
594 and 0.005%) and two plates containing only YMS were prepared. All plates were incubated at 18°C,
595 except for one of the YMS plates that was incubated at 28°C.
596
597 **Phenotypic assay on wheat**

598 Seedlings of the wheat cultivar Obelisk (Wiersum Plantbreeding BV, Winschoten, The Netherlands)
599 were pre-germinated on wet sterile Whatman paper for four days under normal growth conditions (16 h
600 at light intensity of ~200 μmol/m^{-2}s^{-1} and 8 h darkness in growth chambers at 20°C with 90% humidity)
601 followed by potting and further growth for additional seven days. Marked areas on the second leaves
602 (30 leaves per strain) were inoculated with a spore suspension of 10^7 cells/mL in H_2O and 0.1 % Tween
603 20. Mock controls were treated with H_2O and 0.1 % Tween 20 only. 23 days post inoculation treated
604 leaves were analyzed for infection symptoms in form of necrosis and pycnidia. Evaluation was
605 performed by assigning categories for necrosis and pycnidia coverage to each leaf (categories: 0 = 0%,
606 1 = 1-20%, 2 = 21-40%, 3 = 41-60%, 4 = 61-80%, 5 = 81-100%).
607
608 **Analysis of dinucleotide frequencies**

609 TE sequences were extracted from the genome using bedtools getfasta [86]. k-mer frequencies in
610 annotated TEs and masked genomes were determined using the software jellyfish [89].
611 Correspondence analyses were carried out and visualized in R [90] using the packages "FactoMineR"
612 and "factoextra" [91].
613
614 **Mutation accumulation experiment and SNP analysis**

615 A single colony derived directly from a plated dilution of frozen stock for Zt10 or IPO323 was
616 resuspended in 1 mL YMS including 25% glycerol by 2 min vortexing on a VXR basic Vibrax at 2000
617 rpm, and 10–50 μL were re-plated onto a YMS agar plate. Forty replicates were produced. Cells were
618 grown for 7 days at 18°C until a random colony (based on vicinity to a prefixed position on the plate)
619 derived from a single cell was picked and transferred to a new plate as described above. The transfers
620 were conducted for one year (52 times) before the DNA of a randomly chosen colony of each replicate
621 was extracted and sequenced. Sequencing and library preparation were performed at the Max Planck
622 Genome Center in Cologne, Germany (https://mpgc.mpipz.mpg.de/home/). Sequencing was performed
623 on an Illumina HiSeq2500 machine obtaining paired-end 250-nt reads (S9 Table). Paired-end reads
624 were quality filtered (Trimmomatic), mapped (bowtie2) and SNPs were called using samtools mpileup
625 (see text S1).
626
627
628

629 **Data availability**

630 Sequencing raw reads (FASTQ files) of all bisulfite and genomic data and the SMRT genome
631 assemblies generated in this study are available online at Sequence Read Archive (SRA) under
632 BioProject ID PRJNA614493. Previously published genome assemblies are available under BioProject
633 PRJEB33986 [33], PRJNA638605, PRJNA639021 (Zpa63), PRJNA638553 (Zb87), PRJNA638515
634 (Zp13), PRJNA638382 (Za17), https://doi.org/10.5281/zenodo.3820378 [71], PRJNA414407 (Zt05 and
635 Zt10) [36]. The genome sequence of the reference isolate IPO323 (Zt09) is available at:
636 http://genome.jgi.doe.gov/Mycgr3/Mycgr3.home.html [26].

637

638 **Acknowledgements**

639 Research in the lab of EHS is supported by the State of Schleswig-Holstein, the Max Planck Society
640 and CIFAR. Research in the lab of MF is supported by NSF grant (MCB1818006). MM is supported by
641 the German Research Foundation (DFG, MO 3755/1-1). We thank Bruce A. McDonald for providing
642 Iranian *Z. tritici* isolates, Fatemeh Salimi for sampling Iranian *Z. tritici* isolates, and Kathrin Happ, Anja
643 Lachner, and Maja Stralucke for assistance with experiments.

644

645 **Competing Interests**

646 The authors declare no competing interests.

647

References

1. Jones PA. Functions of DNA methylation: Islands, start sites, gene bodies and beyond. Nat Rev Genet. 2012;13: 484–492. doi:10.1038/nrg3230
2. Slotkin RK, Martienssen R. Transposable elements and the epigenetic regulation of the genome. Nat Rev Genet. 2007;8: 272–85. doi:10.1038/nrg2072
3. Martienssen RA, Colot V. DNA Methylation and Epigenetic Inheritance in Plants and Filamentous Fungi. Science. 2001;293: 1070–1074. doi:10.1126/science.293.5532.1070
4. Zemach A, McDaniel IE, Silva P, Zilberman D. Genome-Wide Evolutionary Analysis of Eukaryotic DNA Methylation. Science. 2010;238: 916–919.
5. Lyko F. The DNA methyltransferase family: A versatile toolkit for epigenetic regulation. Nat Rev Genet. 2018;19: 81–92. doi:10.1038/nrg.2017.80
6. Robert M, Morin S, Beaulieu N, Gauthier F, Chute IC, Barsalou A, et al. DNMT1 is required to maintain CpG methylation and aberrant gene silencing in human cancer cells. Nat Genet. 2003;33: 61–65. doi:10.1038/ng1068
7. Gruenbaum Y, Cedar H, Kazin A. Substrate and sequence specificity of a eukaryotic DNA methylase. Nature. 1982;295: 620–622.
8. Leonhardt H, Page AW. A Targeting Sequence Directs DNA Methyltransferase to Sites of DNA Replication in Mammalian. Cell. 1992;71: 865–873.
9. Okano M, Bell DW, Haber DA, Li E. DNA Methyltransferases Dnmt3a and Dnmt3b Are Essential for De Novo Methylation and Mammalian Development. Cell. 1999;99: 247–257.
10. Cao X, Jacobsen SE. Role of the Arabidopsis DRM Methyltransferases in De Novo DNA Methylation and Gene Silencing. Curr Biol. 2002;12: 1138–1144. doi:https://doi.org/10.1016/S0960-9822(02)00925-9
11. Cao X, Springer NM, Muszynski MG, Phillips RL, Kaeppler S, Jacobsen SE. Conserved plant genes with similarity to mammalian de novo DNA methyltransferases. Proc Natl Acad Sci. 2000;97: 4979–4984.
12. Jeltsch A, Jurkowska RZ. New concepts in DNA methylation. Trends Biochem Sci. 2014;39: 310–318. doi:10.1016/j.tibs.2014.05.002
13. Goyal R, Reinhardt R, Jeltsch A. Accuracy of DNA methylation pattern preservation by the Dnmt1 methyltransferase. Nucleic Acids Res. 2006;34: 1182–1188. doi:10.1093/nar/gkl002
14. Zolan ME, Pukkila PJ. Inheritance of DNA methylation in Coprinus cinereus. Mol Cell Biol. 1986;6: 195–200. doi:10.1128/mcb.6.1.195
15. Kouzminova E, Selker EU. Dim-2 encodes a DNA methyltransferase responsible for all known cytosine methylation in Neurospora. EMBO J. 2001;20: 4309–4323. doi:10.1093/emboj/20.15.4309
16. Goll MG, Bestor TH. Eukaryotic Cytosine Methyltransferases. Annu Rev Biochem. 2005;74: 481–514. doi:10.1146/annurev.biochem.74.010904.153721
17. Freitag M, Williams RL, Kothe GO, Selker EU. A cytosine methyltransferase homologue is essential for repeat-induced point mutation in Neurospora crassa. Proc Natl Acad Sci. 2002;99: 8802–8807. doi:10.1073/pnas.132212899
18. Malagnac F, Wendel B, Goyon C, Faugeron G, Zickler D, Rossignol JL, et al. A gene essential for de novo methylation and development in ascobolus reveals a novel type of eukaryotic DNA methyltransferase structure. Cell. 1997;91: 281–290. doi:10.1016/S0092-8674(00)80410-9
19. Gladyshev E, Kleckner N. DNA sequence homology induces cytosine-to-thymine mutation by a heterochromatin-related pathway in Neurospora. Nature Genetics. 2017;49: 887–894. doi:10.1038/ng.3857
20. Huff JT, Zilberman D. Dnmt1-independent CG methylation contributes to nucleosome positioning in diverse eukaryotes. Cell. 2014;156: 1286–1297. doi:10.1016/j.cell.2014.01.029
21. Catania S, Dumesic PA, Pimentel H, Nasif A, Stoddard CI, Burke JE, et al. Evolutionary Persistence of DNA Methylation for Millions of Years after Ancient Loss of a De Novo Methyltransferase. Cell. 2020;180: 263-277.e20. doi:10.1016/j.cell.2019.12.012
22. Bewick AJ, Hofmeister BT, Powers RA, Mondo SJ, Grigoriev IV, James TY, et al. Diversity of cytosine methylation across the fungal tree of life. Nat Ecol Evol. 2019; doi:10.1038/s41559-019-0810-9
23. Ruesch CE, Ramakrishnan M, Park J, Li N, Chong HS, Zaman R, et al. The Histone H3 Lysine 9 Methyltransferase DIM-5 Modifies Chromatin at frequency and Represses Light-Activated Gene Expression. G3: GENES, GENOMES, GENETICS. 2015;5: 93–101.

706 doi:10.1534/g3.114.015446
707 24. Xue Z, Ye Q, Anson SR, Yang J, Xiao G, Kowbel D, et al. Transcriptional interference by
708 antisense RNA is required for circadian clock function. Nature. 2014/08/17. 2014;514: 650–
709 653. doi:10.1038/nature13671
710 25. Dhillon B, Cavaletto JR, Wood KV, Goodwin SB. Accidental amplification and inactivation of a
711 methyltransferase gene eliminates cytosine methylation in Mycosphaerella graminicola.
712 Genetics. 2010;186: 67–77. doi:10.1534/genetics.110.117408
713 26. Goodwin SB, M'barek SB, Dhillon B, Wittenberg AHJ, Crane CF, Hane JK, et al. Finished
714 genome of the fungal wheat pathogen Mycosphaerella graminicola reveals dispensome
715 structure, chromosome plasticity, and stealth pathogenesis. PLOS Genet. 2011;7: e1002070.
716 doi:10.1371/journal.pgen.1002070
717 27. Linde CC, Zhan J, McDonald BA. Population Structure of Mycosphaerella graminicola: From
718 Lesions to Continents. Phytopathology. 2002;92: 946–955. doi:10.1094/PHYTO.2002.92.9.946
719 28. Zhan J, Pettway RE, McDonald BA. The global genetic structure of the wheat pathogen
720 Mycosphaerella graminicola is characterized by high nuclear diversity, low mitochondrial
721 diversity, regular recombination, and gene flow. Fungal Genet Biol. 2003;38: 286–297.
722 doi:10.1016/S1087-1845(02)00538-8
723 29. Hartmann FE, Sánchez-Vallet A, McDonald BA, Croll D. A fungal wheat pathogen evolved host
724 specialization by extensive chromosomal rearrangements. ISME J. 2017;11: 1189–1204.
725 doi:10.1038/ismej.2016.196
726 30. Oggenfuss U, Badet T, Wicker T, Hartmann FE, Singh NK, Abraham LN, et al. A population-
727 level invasion by transposable elements in a fungal pathogen. bioRxiv. 2020;
728 2020.02.11.944652. doi:10.1101/2020.02.11.944652
729 31. Lorrain C, Feurtey A, Möller M, Haueisen J, Stukenbrock E. Dynamics of transposable
730 elements in recently diverged fungal pathogens: lineage-specific transposable element content
731 and efficiency of genome defences. bioRxiv. 2020; 2020.05.13.092635.
732 doi:10.1101/2020.05.13.092635
733 32. Feurtey A, Stevens DM, Stephan W, Stukenbrock EH. Interspecific gene exchange introduces
734 high genetic variability in crop pathogen. Genome Biol Evol. 2019;evz224.
735 doi:10.1093/gbe/evz224
736 33. Badet T, Oggenfuss U, Abraham L, McDonald BA, Croll D. A 19-isolate reference-quality
737 global pangenome for the fungal wheat pathogen Zymoseptoria tritici. BMC Biol. 2020;18: 12.
738 doi:10.1186/s12915-020-0744-3
739 34. Plissonneau C, Stürchler A. The Evolution of Orphan Regions in Genomes of a Fungal
740 Pathogen of Wheat. mBio. 2016;7: e01231-16. doi:10.1128/mBio.01231-16.
741 35. Plissonneau C, Hartmann FE, Croll D. Pangenome analyses of the wheat pathogen
742 Zymoseptoria tritici reveal the structural basis of a highly plastic eukaryotic genome. BMC Biol.
743 2018;16: 5. doi:10.1186/s12915-017-0457-4
744 36. Haueisen J, Möller M, Eschenbrenner CJ, Grandaubert J, Seybold H, Adamiak H, et al. Highly
745 flexible infection programs in a specialized wheat pathogen. Ecol Evol. 2019;9: 275–294.
746 doi:10.1002/ece3.4724
747 37. Stukenbrock EH, Bataillon T, Dutheil JY, Hansen TT, Li R, Zala M, et al. The making of a new
748 pathogen: Insights from comparative population genomics of the domesticated wheat pathogen
749 Mycosphaerella graminicola and its wild sister species. Genome Res. 2011;21: 2157–2166.
750 doi:10.1101/gr.118851.110
751 38. Galagan JE, Selker EU. RIP: The evolutionary cost of genome defense. Trends Genet.
752 2004;20: 417–423. doi:10.1016/j.tig.2004.07.007
753 39. Selker EU. PREMEIOTIC INSTABILITY OF REPEATED SEQUENCES IN NEUROSPORA
754 CRASSA. Annu Rev Genet. 1990;24: 579–613. doi:10.1146/annurev.ge.24.120190.003051
755 40. Möller M, Schotanus K, Soyer JL, Haueisen J, Happ K, Stralucke M, et al. Destabilization of
756 chromosome structure by histone H3 lysine 27 methylation. PLOS Genet. 2019;15: e1008093.
757 doi.org/10.1371/journal.pgen.1008093
758 41. Tamaru H, Selker EU. A histone H3 methyltransferase controls DNA methylation in Neurospora
759 crassa. Nature. 2001;414: 277–83. doi:10.1038/35104508
760 42. Jackson JP, Lindroth AM, Cao X, Jacobsen SE. Control of CpNpG DNA methylation by the
761 KRYPTONITE histone H3 methyltransferase. Nature. 2002;416: 556–560.
762 doi:10.1038/nature731
763 43. Du J, Johnson LM, Jacobsen SE, Patel DJ. DNA methylation pathways and their crosstalk with
764 histone methylation. Nat Rev Mol Cell Biol. 2015;16. doi:10.1038/nrm4043

44. Dumesic PA, Homer CM, Moresco JJ, Pack LR, Shanle EK, Coyle SM, et al. Product Binding Enforces the Genomic Specificity of a Yeast Polycomb Repressive Complex. Cell. 2015;160: 204–218. doi:10.1016/j.cell.2014.11.039
45. Grandaubert J, Bhattacharyya A, Stukenbrock EH. RNA-seq Based Gene Annotation and Comparative Genomics of Four Fungal Grass Pathogens in the Genus Zymoseptoria Identify Novel Orphan Genes and Species-Specific Invasions of Transposable Elements. G3: GENES, GENOMES, GENETICS. 2015;5: g3.115.017731-. doi:10.1534/g3.115.017731
46. Selker EU, Stevens JN. DNA methylation at asymmetric sites is associated with numerous transition mutations. Proc Natl Acad Sci. 1985;82: 8114–8. doi:10.1073/pnas.82.23.8114
47. Holliday R, Grigg GW. DNA methylation and mutation. Mutat Res. 1993;285: 61–67.
48. Stukenbrock EH, Quaedvlieg W, Javan-Nikhah M, Zala M, Crous PW, McDonald BA. Zymoseptoria ardabiliae and Z. pseudotritici, two progenitor species of the septoria tritici leaf blotch fungus Z. tritici (synonym: Mycosphaerella graminicola). Mycologia. 2012;104: 1397–407. doi:10.3852/11-374
49. Quaedvlieg W, Kema GHJ, Groenewald JZ, Verkley GJM, Seifbarghi S, Razavi M, et al. Zymoseptoria gen. nov.: A new genus to accommodate Septoria-like species occurring on graminicolous hosts. Persoonia Mol Phylogeny Evol Fungi. 2011;26: 57–69. doi:10.3767/003158511X571841
50. McDonald MC, McGinness L, Hane JK, Williams AH, Milgate A, Solomon PS. Utilizing Gene Tree Variation to Identify Candidate Effector Genes in Zymoseptoria tritici. G3: GENES, GENOMES, GENETICS. 2016;6: 779–91. doi:10.1534/g3.115.025197
51. Montanini B, Chen P-Y, Morselli M, Jaroszewicz A, Lopez D, Martin F, et al. Non-exhaustive DNA methylation-mediated transposon silencing in the black truffle genome, a complex fungal genome with massive repeat element content. Genome Biol. 2014;15: 411. doi:10.1186/s13059-014-0411-5
52. Nakayashiki H, Ikeda K, Hashimoto Y, Tosa Y, Mayama S. Methylation is not the main force repressing the retrotransposon MAGGY in Magnaporthe grisea. Nucleic Acids Res. 2001;29: 1278–84. doi:10.1093/nar/29.6.1278
53. Duncan BK, Miller JH. Mutagenic deamination of cytosine residues in DNA. Nature. 1980;287: 560–561. doi:10.1038/287560a0
54. Kiefer C, Willing E, Jiao W, Sun H, Piednoël M, Hümann U, et al. Interspecies association mapping links reduced CG to TG substitution rates to the loss of gene body methylation. Nat Plants. 2019;5. doi:10.1038/s41477-019-0486-9
55. Mazur AK, Gladyshev E. Partition of Repeat-Induced Point Mutations Reveals Structural Aspects of Homologous DNA-DNA Pairing. Biophys J. 2018;115: 605–615. doi:10.1016/j.bpj.2018.06.030
56. Yang AS, Shen JC, Zingg JM, Mi S, Jones PA. HhaI and HpaII DNA methyltransferases bind DNA mismatches, methylate uracil and block DNA repair. Nucleic Acids Res. 1995;23: 1380–1387. doi:10.1093/nar/23.8.1380
57. Shen JC, Zingg JM, Yang AS, Schmutte C, Jones PA. A mutant HpaII methyltransferase functions as a mutator enzyme. Nucleic Acids Res. 1995;23: 4275–4282. doi:10.1093/nar/23.21.4275
58. Rosa AL, Folco HD, Mautino MR. In vivo levels of S-adenosylmethionine modulate C:G to T:A mutations associated with repeat-induced point mutation in Neurospora crassa. Mutat Res Mol Mech Mutagen. 2004;548: 85–95. doi:https://doi.org/10.1016/j.mrfmmm.2004.01.001
59. Mautino MR, Rosa AL. Analysis of Models Involving Enzymatic Activities for the Occurrence of C→T Transition Mutations During Repeat-Induced Point Mutation (RIP) in Neurospora crassa. J Theor Biol. 1998;192: 61–71. doi:https://doi.org/10.1006/jtbi.1997.0608
60. Chen L, MacMillan AM, Verdine GL. Mutational separation of DNA binding from catalysis in a DNA cytosine methyltransferase. J Am Chem Soc. 1993;115: 5318–5319. doi:10.1021/ja00065a063
61. Shen J-C, Rideout III WM, Jones PA. High frequency mutagenesis by a DNA methyltransferase. Cell. 1992;71: 1073–1080. doi:10.1016/S0092-8674(05)80057-1
62. Wang K-Y, James Shen C-K. DNA methyltransferase Dnmt1 and mismatch repair. Oncogene. 2004;23: 7898–7902. doi:10.1038/sj.onc.1208111
63. Freitag M. Histone Methylation by SET Domain Proteins in Fungi. Annu Rev Microbiol. 2017;36: 413–439. doi:10.1146/annurev-micro-102215-095757
64. Ikeda KI, Van Vu B, Kadotani N, Tanaka M, Murata T, Shiina K, et al. Is the fungus Magnaporthe losing DNA methylation? Genetics. 2013;195: 845–855.

824 doi:10.1534/genetics.113.155978
825 65. Yang K, Liang L, Ran F, Liu Y, Li Z, Lan H, et al. The DmtA methyltransferase contributes to
826 Aspergillus flavus conidiation, sclerotial production, aflatoxin biosynthesis and virulence. Sci
827 Rep. 2016;6: 1–13. doi:10.1038/srep23259
828 66. Selmecki A, Forche A, Berman J. Genomic plasticity of the human fungal pathogen Candida
829 albicans. Eukaryot Cell. 2010;9: 991–1008. doi:10.1128/EC.00060-10
830 67. Hu G, Wang J, Choi J, Jung WH, Liu I, Litvintseva AP, et al. Variation in chromosome copy
831 number influences the virulence of Cryptococcus neoformans and occurs in isolates from AIDS
832 patients. BMC Genomics. 2011;12: 526. doi:10.1186/1471-2164-12-526
833 68. Möller M, Stukenbrock EH. Evolution and genome architecture in fungal plant pathogens. Nat
834 Rev Microbiol. 2017;15: 756. doi.org/10.1038/nrmicro.2017.76
835 69. Raffaele S, Kamoun S. Genome evolution in filamentous plant pathogens: why bigger can be
836 better. Nat Rev Microbiol. 2012;10: 417–430. doi:10.1038/nrmicro2790
837 70. Allen GC, Flores-Vergara MA, Krasynanski S, Kumar S, Thompson WF. A modified protocol for
838 rapid DNA isolation from plant tissues using cetyltrimethylammonium bromide. Nat Protoc.
839 2006;1: 2320–2325. doi:10.1038/nprot.2006.384
840 71. Feurtey A, Lorrain C, Croll D, Eschenbrenner C, Freitag M, Habig M, et al. Genome
841 compartmentalization predates species divergence in the plant pathogen genus Zymoseptoria.
842 BMC Genomics. 2020;21: 588. doi:10.1186/s12864-020-06871-w
843 72. Flutre T, Duprat E, Feuillet C, Quesneville H. Considering Transposable Element
844 Diversification in De Novo Annotation Approaches. PLoS One. 2011;6: e16526.
845 doi:10.1371/journal.pone.0016526
846 73. Bolger AM, Lohse M, Usadel B. Trimmomatic: A flexible trimmer for Illumina sequence data.
847 Bioinformatics. 2014;30: 2114–2120. doi:10.1093/bioinformatics/btu170
848 74. Kim D, Langmead B, Salzberg SL. HISAT: a fast spliced aligner with low memory
849 requirements. Nat Methods. 2015;12: 357–60. doi:10.1038/nmeth.3317
850 75. Jin Y, Hammell M. Analysis of RNA-Seq Data Using TE transcripts. Methods Mol Biol.
851 2018;1751: 153–167. doi:10.1007/978-1-4939-7710-9_11
852 76. Stukenbrock EH, Dutheil JY. Fine-scale recombination maps of fungal plant pathogens reveal
853 dynamic recombination landscapes and intragenic hotspots. Genetics. 2018;208: 1209–1229.
854 doi:10.1534/genetics.117.300502
855 77. Möller M, Habig M, Freitag M, Stukenbrock EH. Extraordinary Genome Instability and
856 Widespread Chromosome Rearrangements During Vegetative Growth. Genetics. 2018;210 no.
857 2: 517–529. doi:10.1534/genetics.118.301050
858 78. Grandaubert J, Dutheil JY, Stukenbrock EH. The genomic determinants of adaptive evolution
859 in a fungal pathogen. Evolution Letters. 2019; 299–312. doi:10.1002/evl3.117
860 79. Jürgens T, Linde CC, Mcdonald BA. Genetic structure of Mycosphaerella graminicola
861 populations from Iran, Argentina and Australia. Eur J Plant Pathol. 2006; 115:223–23.
862 doi:10.1007/s10658-006-9000-0
863 80. Daboussi MJ. Fungal transposable elements and genome evolution. Genetica. 1997;100: 253–
864 260. doi:10.1023/A:1018354200997
865 81. Zhan J, Linde CC, Jürgens T, Merz U, Steinebrunner F, McDonald BA. Variation for neutral
866 markers is correlated with variation for quantitative traits in the plant pathogenic fungus
867 Mycosphaerella graminicola. Mol Ecol. 2005;14: 2683–2693. doi:10.1111/j.1365-
868 294X.2005.02638.x
869 82. Kearse M, Moir R, Wilson A, Stones-Havas S, Cheung M, Sturrock S, et al. Geneious Basic:
870 An integrated and extendable desktop software platform for the organization and analysis of
871 sequence data. Bioinformatics. 2012;28: 1647–1649. doi:10.1093/bioinformatics/bts199
872 83. Poppe S, Dorsheimer L, Happel P, Stukenbrock EH. Rapidly Evolving Genes Are Key Players
873 in Host Specialization and Virulence of the Fungal Wheat Pathogen Zymoseptoria tritici
874 (Mycosphaerella graminicola). PLOS Pathog. 2015;11: 1–21.doi:10.1371/journal.ppat.1005055
875 84. Gibson DG, Young L, Chuang RY, Venter JC, Hutchison CA, Smith HO. Enzymatic assembly
876 of DNA molecules up to several hundred kilobases. Nat Methods. 2009;6: 343–345.
877 doi:10.1038/nmeth.1318
878 85. Krueger F, Andrews SR. Bismark: a flexible aligner and methylation caller for Bisulfite-Seq
879 applications. Bioinformatics. 2011;27: 1571–1572. doi:10.1093/bioinformatics/btr167
880 86. Quinlan AR, Hall IM. BEDTools: a flexible suite of utilities for comparing genomic features.
881 Bioinformatics. 2010;26: 841–842. doi.org/10.1093/bioinformatics/btq033
882 87. Southern EM. Detection of specific sequences among DNA fragments separated by gel

electrophoresis. J Mol Biol. 1975;98: 503–517. doi:10.1016/S0022-2836(75)80083-0
88. Sambrock J, W. Russel D. Molecular Cloning: A Laboratory Manual(3rd edition). 2001
89. Marçais G, Kingsford C. A fast, lock-free approach for efficient parallel counting of occurrences of k-mers. Bioinformatics. 2011;27: 764–770. doi:10.1093/bioinformatics/btr011
90. R Core Team. R: A Language and Environment for Statistical Computing. R Found Stat Comput. 2019; Available: https://www.r-project.org
91. Lê S, Josse J, Husson F. FactoMineR: An R Package for Multivariate Analysis. J Stat Software. 2008, Vol 25, Issue 1; doi:10.18637/jss.v025.i01
92. Letunic I, Bork P. 20 years of the SMART protein domain annotation resource. Nucleic Acids Res. 2017;46: D493–D496. doi:10.1093/nar/gkx922
93. Finn RD, Attwood TK, Babbitt PC, Bateman A, Bork P, Bridge AJ, et al. InterPro in 2017-beyond protein family and domain annotations. Nucleic Acids Res. 2017;45: D190–D199. doi:10.1093/nar/gkw1107

897 **Supplementary Information**

898

899 **Supplementary Tables**

900

901 **S1 Table.** List of *Z. tritici*, *Z. ardabiliae*, *Z. brevis* and *Z. passerinii* isolates used in this study.
902 Listed are collection date, origin, information about the genome assembly and
903 presence/absence of *dim2* in each isolate.

904

905 **S2 Table.** Detected copies and pairwise identity of full-length (>3,000 bp) *dim2* copies in *Z.*
906 *tritici* genomes. The *dim2* gene of the Iranian isolate Zt469 was used as query for the blast
907 search.

908

909 **S3 Table.** Dinucleotide frequencies in transposable elements (TEs) and TE masked genomes
910 in *Z. tritici* isolates and the sister species *Z. brevis*, *Z. ardabiliae* and *Z. passerinii*.

911

912 **S4 Table.** Genes overlapping TEs and their functional annotation in Zt09.

913

914 **S5 Table.** SNPs detected in Zt10 and IPO323 after 52 weeks of experimental evolution
915 compared to the reference strain at the start of the experiment.

916

917 **S6 Table.** Genome-wide occurrence of 5mC and SNPs in Zt10. Listed are GC and AT content,
918 number of 5mC sites (pooled data from WGBS of all three replicates) and number of SNPs
919 (pooled data from all 40 replicates) in 500 bp windows.

920

921 **S7 Table.** PacBio genome assembly metrics of Iranian isolates Zt289 and Zt469.

922

923 **S8 Table.** List of all oligos and plasmids used in this study.

924

925 **S9 Table.** Overview of Illumina sequencing data, detected 5mC sites, and SNPs.

926

927 **Supplementary text S1.** Software and commands used for bisulfite and genome data analysis
928 to detect 5mC sites and SNPs.

929 **Supplementary Figures**

930

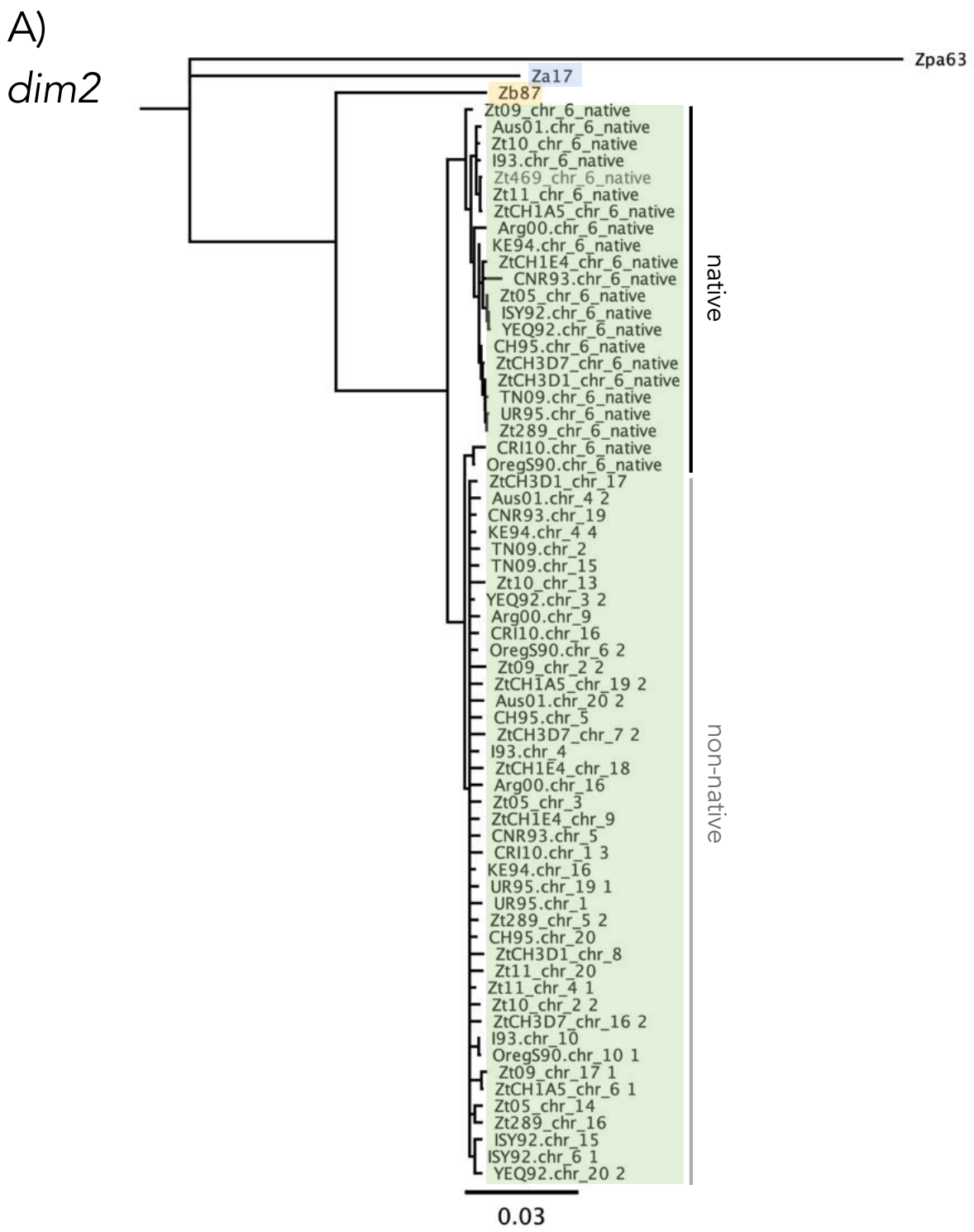

931

B) *dnmt5*

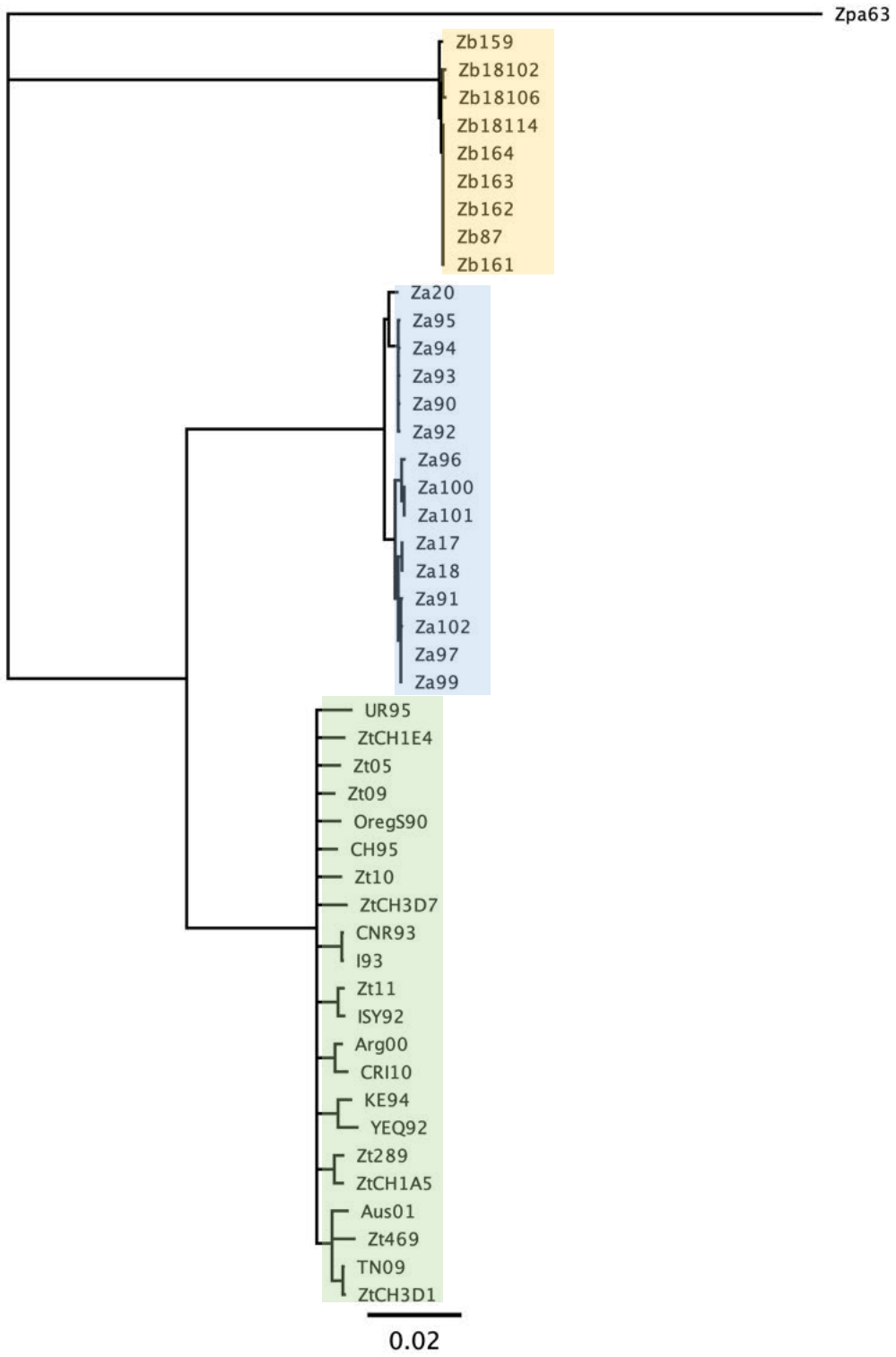
Zpa63
Zb159
Zb18102
Zb18106
Zb18114
Zb164
Zb163
Zb162
Zb87
Zb161
Za20
Za95
Za94
Za93
Za90
Za92
Za96
Za100
Za101
Za17
Za18
Za91
Za102
Za97
Za99
UR95
ZtCH1E4
Zt05
Zt09
OregS90
CH95
Zt10
ZtCH3D7
CNR93
I93
Zt11
ISY92
Arg00
CRI10
KE94
YEQ92
Zt289
ZtCH1A5
Aus01
Zt469
TN09
ZtCH3D1
0.02

932

C) *rid*

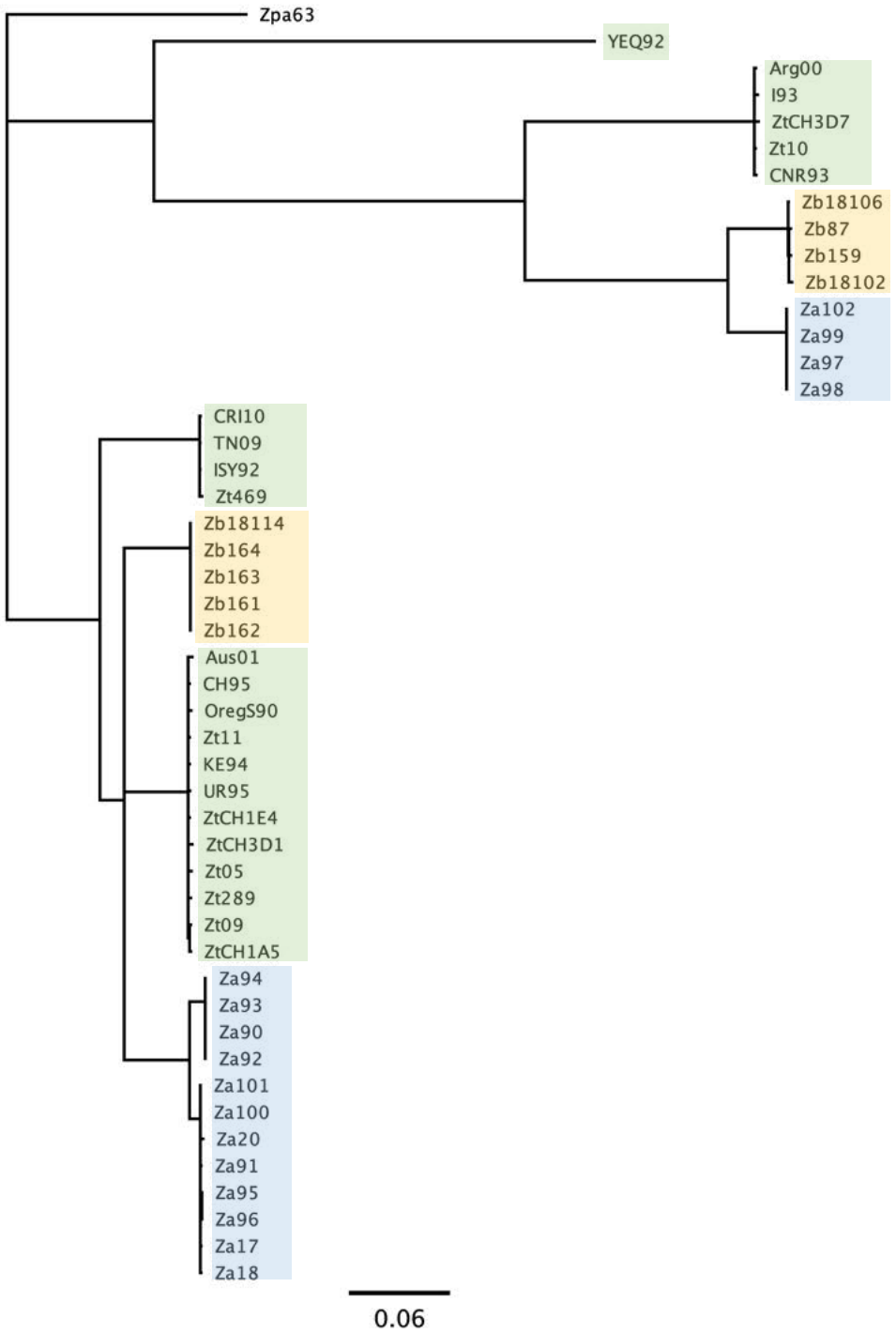

S1 Fig. Phylogenetic trees of DNA sequences encoding the *dim2*, *dnmt5*, and *rid* genes. **A)** Phylogenetic tree based on alignments of "deRIPed" *dim2* alleles to the native, functional gene of Zt469. The *Z. tritici dim2* is distinct from the *Z. brevis* and *Z. ardabiliae* gene. The native *Z. tritici* copies, except for OregS90 and CRI10, and non-native copies form distinct clusters. Shown are two representative non-native copies per isolate. **B)** *Dnmt5* is present in all analyzed genomes and shows relatively little inter- or intraspecies diversity. **C)** The *rid gene* shows an exceptionally high inter- and intraspecies diversity with three highly distinct alleles present among genomes of *Z. tritici*, *Z. ardabiliae* and *Z. brevis*. Green background indicates *Z. tritici*, blue *Z. ardabiliae*, yellow *Z. brevis*. *Z. passerinii* is used as an outgroup.

A
original sequences
1
1000
2000
3000
native
non-native
intact
recently
mutated
non-functional
intact
recently
mutated
non-functional

944

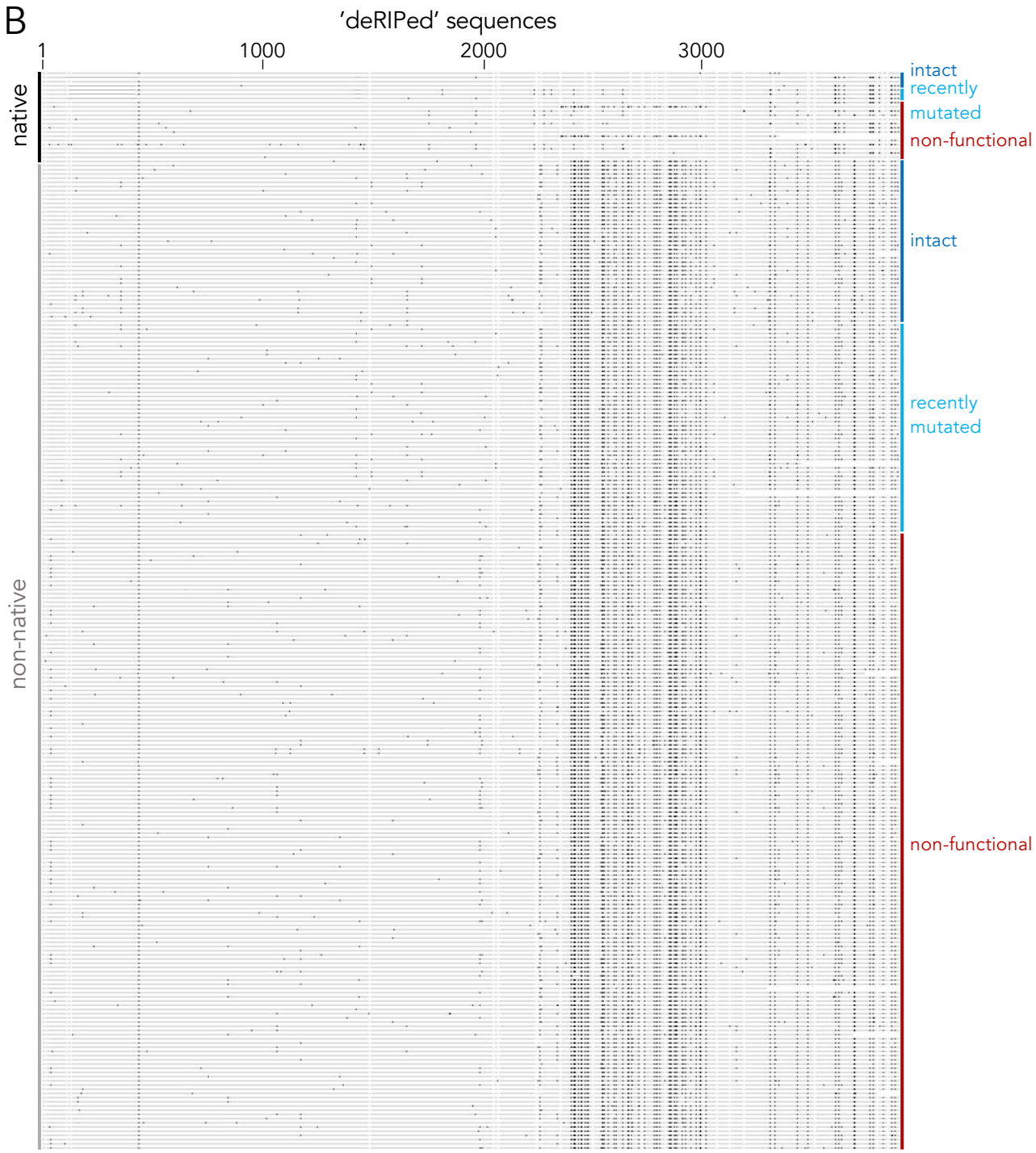

S2 Fig. Alignment of original **(A)** and 'deRIPed' **(B)** full-length (> 3000 bp) *dim2* alleles compared to the functional allele of isolate Zt469. All native copies, (functional and non-functional, except for OregS90 and CRI10) lack mutations in the DNA methyltransferase domain (position ~2,300–3,500) that are present in all non-native copies suggesting that the additional copies did not emerge from amplification of the native *dim2*. Black lines indicate differences to the reference.

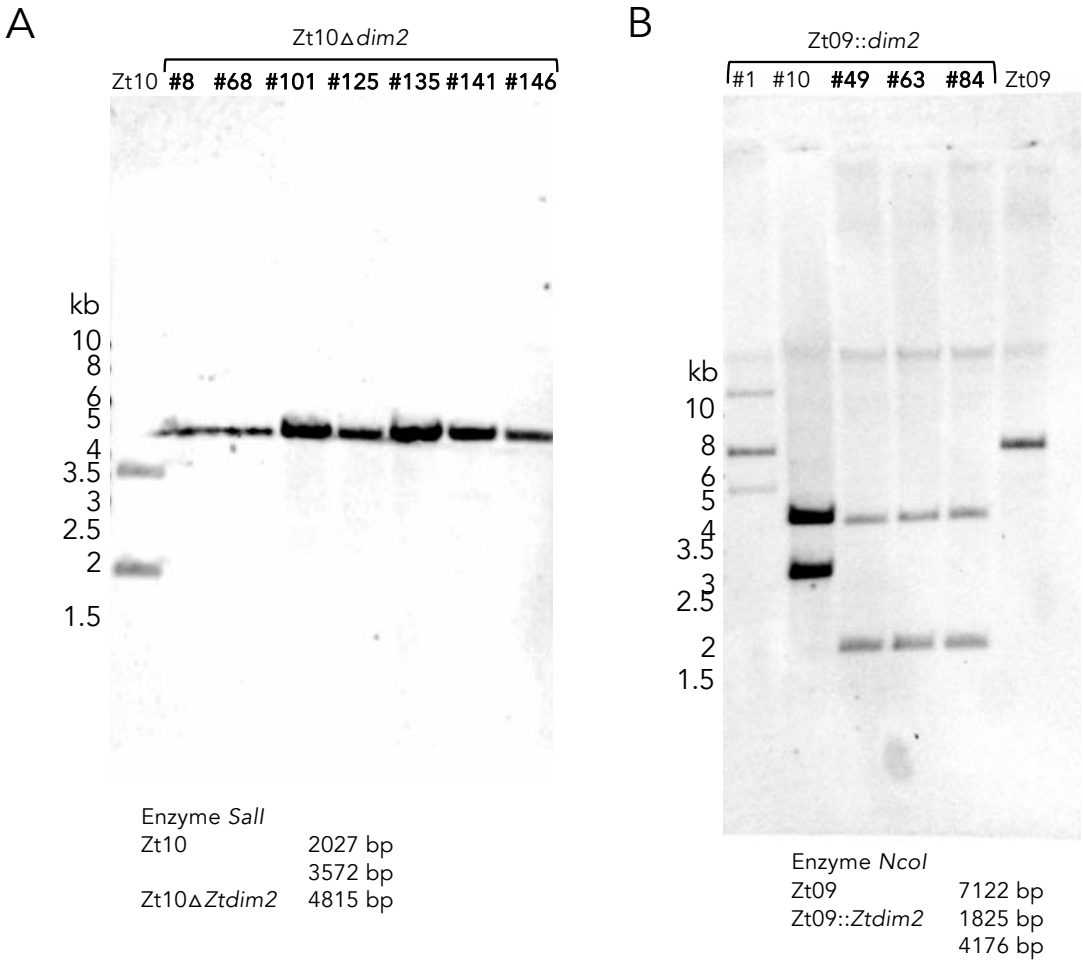

S3 Fig. Southern blots to confirm the correct integration of **A)** the deletion construct for *dim2* in Zt10 (Zt10Δ*dim2*) and **B)** *dim2* (originating from Zt10) in Zt09 (Zt09::*dim2*). Three positive transformants (#49, #63 and #84) were found amongst the Zt09::*dim2* candidates, whereas all seven candidates for Zt10Δ*dim2* were verified (correct transformants are highlighted in bold).

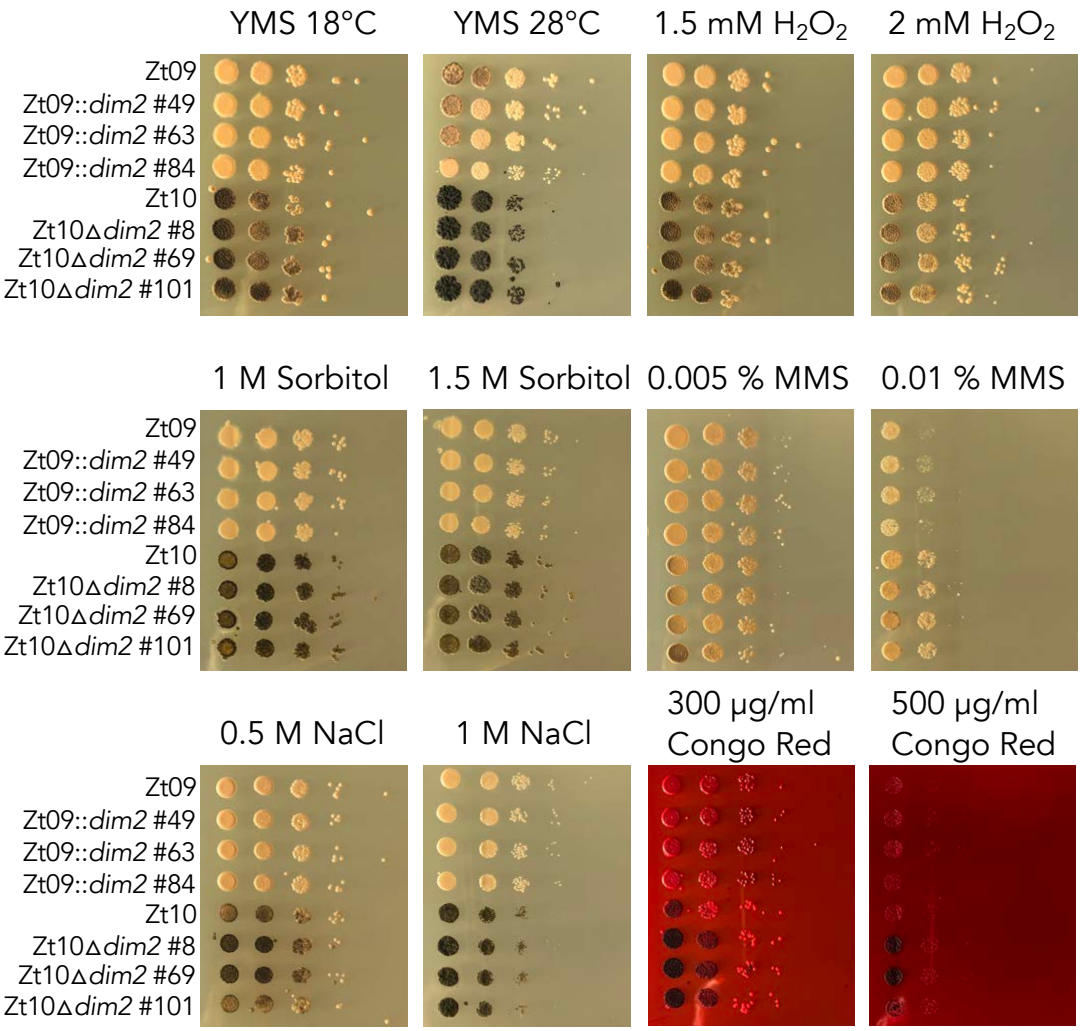

S4 Fig. Phenotypic characterization of Zt10, Zt10Δ*dim2*, Zt09 and Zt09::*dim2 in vitro*. We compared growth phenotypes under different *in vitro* conditions including temperature, osmotic, oxidative, genotoxic and cell wall stress. We spotted spore dilutions of each reference isolate and three independent *dim2* mutant transformants on each plate. We did not detect any noticeable differences in growth between reference and mutant strains but differences between the different *Z. tritici* isolates Zt09 and Zt10 that were previously described [36].

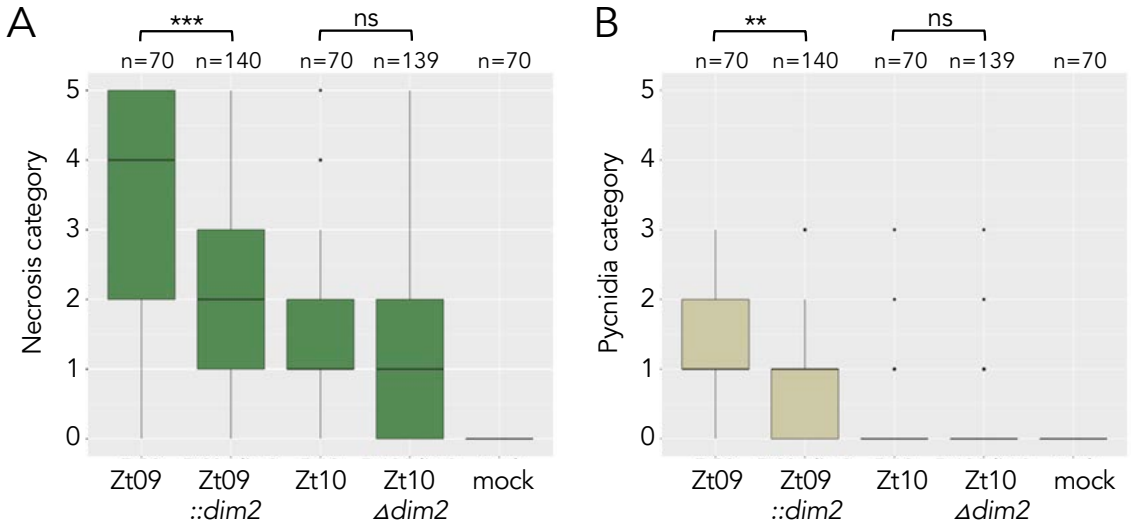

968

969

970 **S5 Fig.** Results of wheat infection experiments with *Z. tritici* isolates Zt09, Zt10 and the mutants
971 Zt09::*dim2* and Zt10Δ*dim2* on wheat. **A)** Zt09*::dim2* strains show significantly less necrotic lesions
972 compared to Zt09 (*** Wilcoxon rank-sum test, *p*-value = 2.178 x 10^{-7}) while there is no significant
973 difference in the quantities of necrotic lesions caused by Zt10 and Zt10Δ*dim2* strains. **B)** Coverage with
974 pycnidia is significantly reduced between Zt09 and Zt09*::dim2* (** *p*-value = 0.003301) but not between
975 Zt10 and Zt10Δ*dim2* strains. Categories for necrotic lesion and pycnidia coverage: 0 = 0%, 1 = 1-20%,
976 2 = 21-40%, 3 = 41-60%, 4 = 61-80%, 5 = 81-100%.

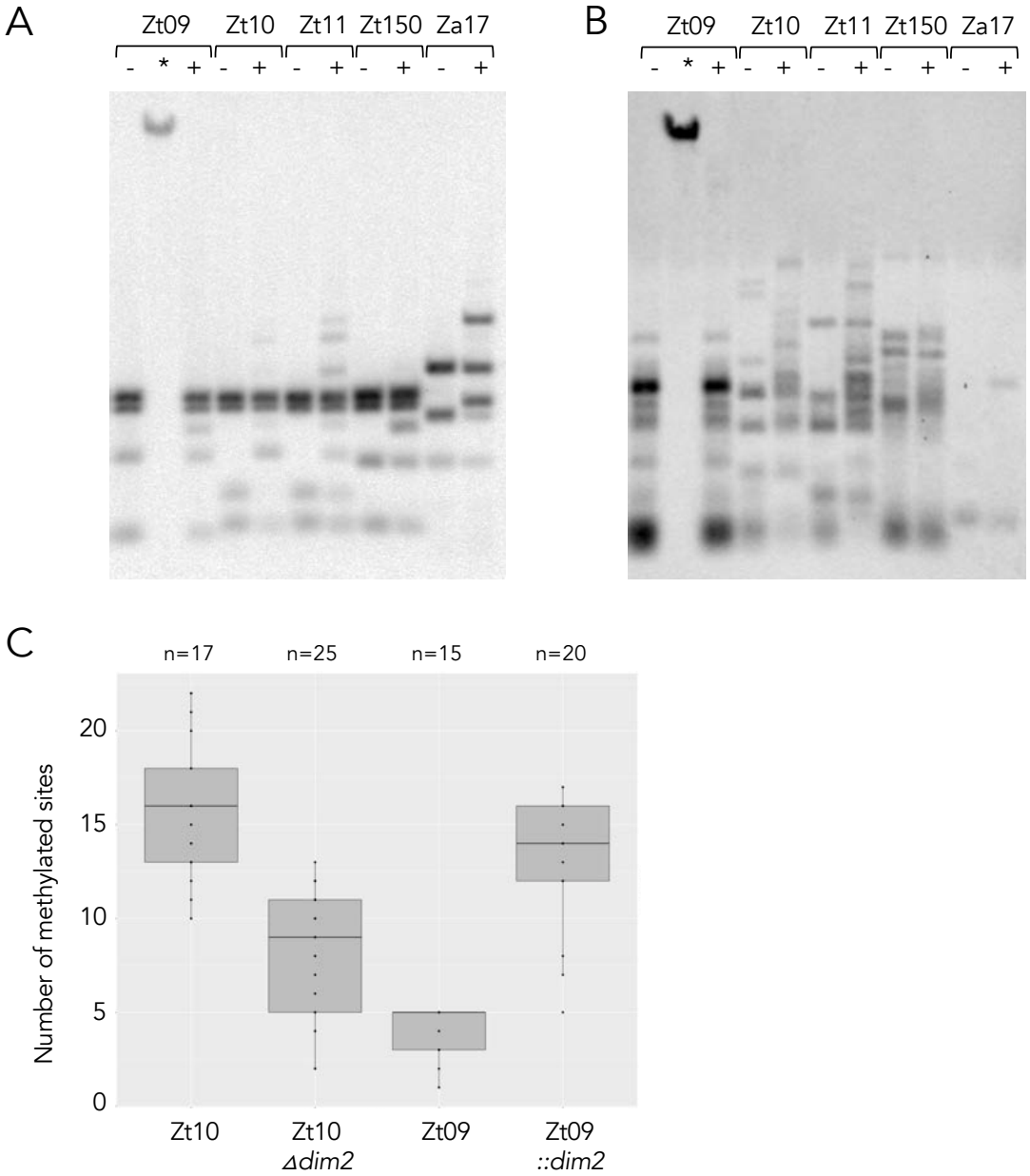

977

978 **S6 Fig. Detection of cytosine methylation by enzymatic digestion and Southern blot and**
979 **confirmation of bisulfite sequencing results by PCR and Sanger sequencing.** Restriction enzyme
980 analysis followed by Southern blots using the rDNA spacer **(A)** or a retrotransposon RIL2 **(B)** as probe.
981 In addition to the cytosine methylation sensitive (*Bfu*CI, **+**) or insensitive (*Dpn*II, **-**) enzymes, we used
982 *Dpn*I (*****) to test for the presence of adenine methylation. Zt09 and Zt150 contain a non-functional *dim2*,
983 whereas the Iranian strains Zt10, Zt11 and the *Z. ardabiliae* strain Za17 have an intact copy. In all strains
984 with a functional *dim2* we see a clear difference between the restrictions with *Bfu*CI and *Dpn*II, indicating
985 the presence of DNA methylation. In Zt09 and Zt150 this difference is not detectable except for one
986 band that is not restricted in both strains in the rDNA blot. The genomic DNA of Zt09 treated with *Dpn*I
987 is not digested suggesting absence of 6mA methylation in these regions. **C)** Confirmation of bisulfite
988 sequencing by an independent bisulfite treatment followed by PCR of target loci and Sanger
989 sequencing. Two target loci (repeated region that showed 5mC signals in all isolates) were chosen per
990 isolate, shown are the number of detected 5mC sites in these loci (size of loci ~ 180 – 260 bp). N is the
991 number of cloned PCR products that were sequenced. Based on these data we can confirm the
992 presence of 5mC methylation in all isolates and a lower frequency in absence of *dim2*.

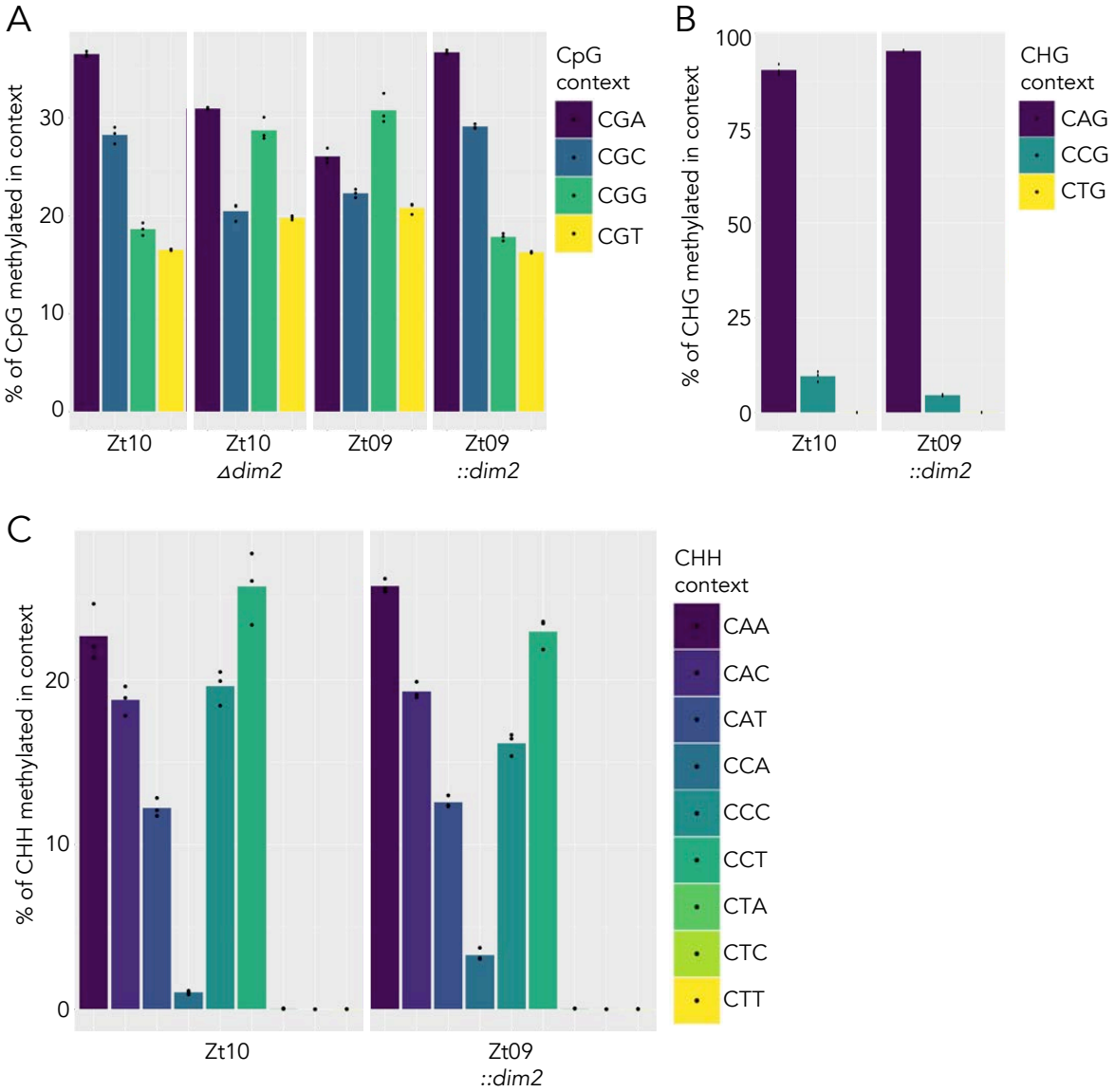

S7 Fig. 5mC site preferences in CG, CHG and CHH sequence contexts. **A)** CGA and CGC sites are preferred in CG contexts in presence of *dim2*, while CGA and CGG are slightly preferred targets in absence of *dim2*. **B)** Among CHG sites, CAG sites are the predominant target sites of 5mC. For CHG and CHH contexts only data for Zt10 and Zt09::*dim2* are shown, as there is no detectable methylation outside of CG contexts in absence of *dim2*. **C)** In CHH contexts, CA sites followed by CC sites have the highest methylation frequency. CT sites are almost completely devoid of 5mC.

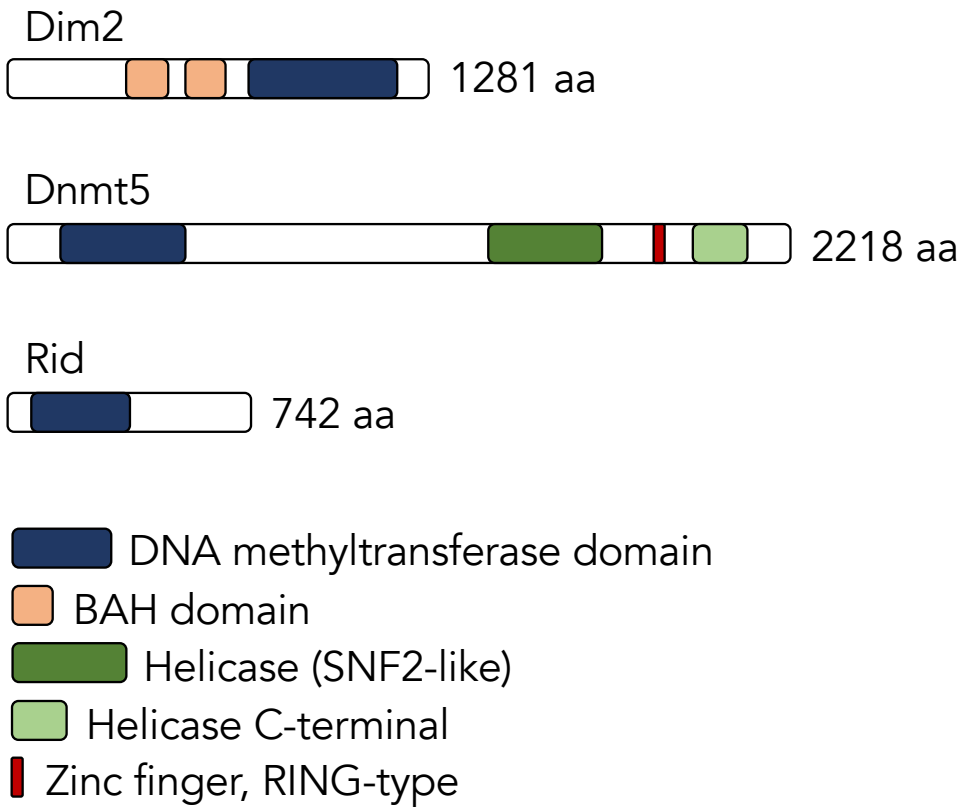

S8 Fig. Predicted domains of the three putative DNA methyltransferase proteins Dim2, Dnmt5 and Rid identified in the *Zymoseptoria* genomes. Protein sequences were analyzed with SMART [92], NCBI Blast and InterProScan [93].